Chapter 4
Second-Order Sliding Mode Controllers and Differentiators

As we have seen, classic sliding modes provide robust and high-accuracy solutions for a wide range of control problems under uncertainty conditions. However, two main restrictions remain. First, the constraint to be held at zero in conventional sliding modes has to be of relative degree 1, which means that the control needs to explicitly appear in the first time derivative of the constraint. Thus, one has to search for an appropriate constraint. Second, high-frequency control switching may easily cause unacceptable practical complications (chattering effect), if the control has any physical sense.

Suppose that the problem is to keep the sliding variable s at zero, while the control appears only in $\ddot{s}$. Usually the constraint function $\sigma = s + \dot{s}$ is chosen. By construction, $\dot{\sigma} = \dot{s} + \ddot{s}$ contains the control, and σ can be kept at zero in a classic sliding mode (Chap. 2). As a result s tends asymptotically to zero. Keeping it at exact zero is not possible. One also needs to calculate $\dot{s}$ to realize this scheme. Both of these goals, exact robust differentiation and exactly keeping $s = 0$, can be accomplished by the second-order sliding mode technique to be developed in this chapter.

Suppose that the problem is to keep s at zero, while the control appears already in $\dot{s}$. This problem is easily solved by means of conventional sliding modes (Chap. 2). But often the chattering effect makes the solution unacceptable. A possible solution is to consider the control derivative as a new virtual control. Then the above reasoning can be applied, and using a second-order sliding mode technique, the task can be accomplished exactly, and in finite time, by means of *continuous* control. As a consequence it can be expected that the chattering effect is significantly attenuated.

4.1 Introduction

Consider a simple control system involving target pointing by means of a pendulum (with the angle coordinate measured from $q = \pi/6$) given by

$$\dot{x} = -\sin(x + q) + u,\ q = \pi/6 \tag{4.1}$$

Y. Shtessel et al., *Sliding Mode Control and Observation*, Control Engineering,
DOI 10.1007/978-0-8176-4893-0_4,

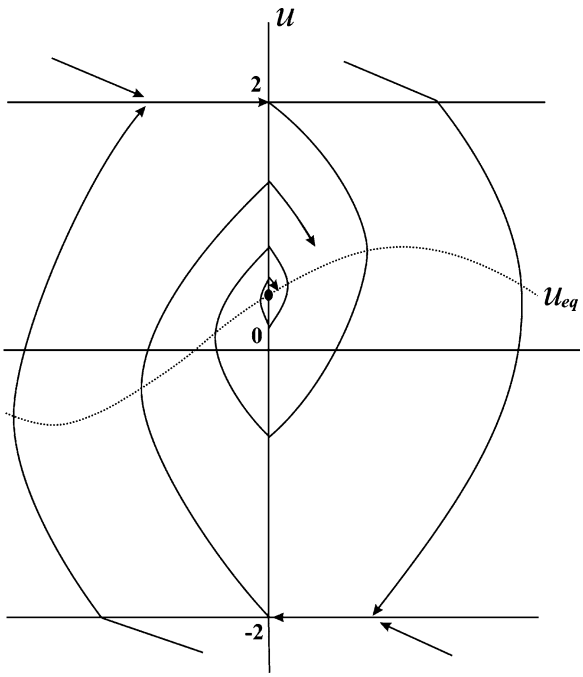

Fig. 4.1 Asymptotically stable second-order sliding mode at $x = 0, u = \sin(q)$

The targeting problem is reformulated as the stabilization of Eq. (4.1) at $x = 0$. It is easily solved by means of the standard relay controller

$$u = -2\,\mathrm{sign}(x) \tag{4.2}$$

As we have already seen, this controller produces considerable chattering. One of the natural ways to avoid chattering is to introduce dynamical regularization gradually switching the control

$$\dot{u} = \begin{cases} -u & \text{if } |u| > 2 \\ -\alpha\,\mathrm{sign}(x) & \text{if } |u| \le 2 \end{cases} \tag{4.3}$$

where $u(0) = u_0$.

Let x and u be the new coordinates (Fig. 4.1), and suppose α is sufficiently large. Obviously, we get $\dot{x} > 0$ with $u > u_{eq} = \sin(x + \pi/6)$ and $\dot{x} < 0$ with $u < \sin(x + q)$. Each trajectory starting from the point $(0, u_0)$, with $u_0 > \sin(q) = \sin(\pi/6) = 0.5$, revolves around the point $(0, 0.5)$. The closer is the initial point to $(0, 0.5)$, the closer is the trajectory to $(0, 0.5)$. Thus the point $(0, 0.5)$ is the *limit of trajectories*. Furthermore it can even be shown that solutions asymptotically converge to this point. From the theory of ordinary differential equations one learns that a limit trajectory also has to be a solution trajectory. In other words,

$x = 0, u = 0.5$ is a constant solution of the system (4.1), (4.3). Moreover, obviously the solution should still be $x = 0, u = \sin(q)$, with q slowly changing. The point $x = 0, u = 0.5$ does not represent a solution in any classical sense, but is a solution in the sense of Filippov.

The point $x = 0, u = \sin(q) = 0.5$ satisfies the conditions

$$x = 0, \dot{x} = 0 \tag{4.4}$$

Such a constant solution would be an ideal solution for the stated control problem, provided it can indeed be considered as a solution of Eqs. (4.1), (4.3). Motions satisfying (4.4) are said to be in *the second-order sliding mode* or 2-*sliding mode*. The point $x = 0$, $u = 0.5$ is the 2-*sliding manifold*. In this chapter we will learn how to establish such modes and to ensure their *finite-time stability*. But first we need to redefine the very notion of the solution for the case of differential equations with discontinuous right-hand sides.

Definition 4.1. Consider a discontinuous differential equation $\dot{x} = f(x)$ (Filippov differential inclusion $\dot{x} \in F(x)$) with a smooth output function $\sigma = \sigma(x)$, and let it be understood in the Filippov sense. Then, provided that:

1. σ and the total time derivative $\dot{\sigma} = \sigma'_x(x) f(x)$ are continuous functions of x
2. The set

$$\sigma = \dot{\sigma} = 0 \tag{4.5}$$

   is a nonempty integral set
3. The Filippov set of admissible velocities at the set defined by Eq. (4.5) contains more than one vector

the motion on the set (4.5) is said to exist in a 2-sliding (second-order sliding) mode (Fig. 4.2), and the set (4.5) is called a 2-sliding set. The nonautonomous case is reduced to the considered one by introducing the fictitious equation $\dot{t} = 1$.

Note that the third requirement means that set (4.5) is a discontinuity set of the equation, and it is introduced here only to exclude extraneous cases of integral manifolds of continuous differential equations. That condition is illustrated by the two limit velocity vectors at the 2-sliding point M in Fig. 4.2. Also note that the extension of the above definitions by the introduction of the fictitious equation $\dot{t} = 1$ actually makes time similar to other coordinates. This approach is different from the standard definition by Filippov, it is simpler, and it provides for more solutions.

The conventional sliding mode described in Chap. 2 is called first order (σ is continuous, and $\dot{\sigma}$ is discontinuous). The general definition of the sliding mode order is very similar and is introduced in Chap. 6.

Remark 4.1. The notion of the sliding order appears to be connected with the notion of relative degree.

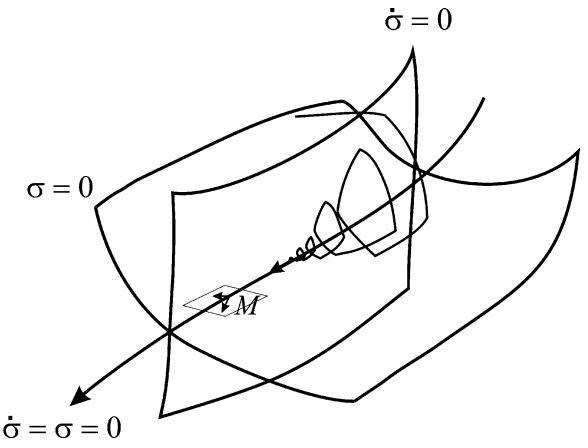

Fig. 4.2 2-sliding mode

Consider a general system linear in the control given by

$$\dot{x} = a(t,x) + b(t,x)u \tag{4.6}$$

$x \in \mathbb{R}^n$, with the output

$$\sigma = \sigma(t,x) \tag{4.7}$$

The functions a, b, σ are assumed to have all the necessary derivatives. In this chapter we consider the simplest case when $\sigma, u \in \mathbb{R}$. The total time derivative of σ is defined as

$$\dot{\sigma} = \sigma'_t + \sigma'_x a + \sigma'_x bu$$

Suppose that $\sigma'_x b \equiv 0$. Then calculating the second total derivative yields

$$\ddot{\sigma} = \sigma''_{tt} + 2\sigma''_{tx}a + \sigma'_x a'_t + [\sigma''_{xx}(a+bu)]a + \sigma'_x[a'_x(a+bu)]$$

Thus,

$$\ddot{\sigma} = h(t,x) + g(t,x)u,\ g(t,x) = (\sigma''_{xx}b)a + \sigma'_x(a'_x b) \tag{4.8}$$

where h is another appropriately defined function. Hence, the relative degree equals 1 if $\sigma'_x b \neq 0$, and it equals 2 , if $\sigma'_x b \equiv 0$ and $(\sigma''_{xx}b)a + \sigma'_x(a'_x b) \neq 0$.

Suppose that the system relative degree exists, and the control function u is defined by some discontinuous feedback. Then with relative degree 1 the function $\dot{\sigma}$ is discontinuous, while σ of course is continuous. On the other hand with relative degree 2 and discontinuous u get that σ, $\dot{\sigma}$ are continuous functions, while $\ddot{\sigma}$ is discontinuous. Therefore we come to conclusion that the conventional sliding (1-sliding) mode can only be achieved with relative degree 1, while the second-order sliding (2-sliding) mode requires relative degree 2 with respect to discontinuous control.

4.2 2-Sliding Mode Controllers

Once more consider a dynamic system of the form

$$\dot{x} = a(t,x) + b(t,x)u,\ \sigma = \sigma(t,x) \tag{4.9}$$

where $x \in \mathbb{R}^n$, $u \in \mathbb{R}$ is control, σ is the only measured output, and the smooth functions a, b, σ (and the dimension n) are unknown. The task is to make the output σ vanish in finite time and to keep $\sigma \equiv 0$ by means of discontinuous globally bounded feedback control. The system trajectories are supposed to be infinitely extendible in time for any bounded input. The system is understood in the Filippov sense.

Assume that the measured output $\sigma(t,x)$ is twice differentiable with respect to time and the condition $\sigma'_x b \equiv 0$ and $(\sigma''_{xx}b)a + \sigma'_x(a'_x b) \neq 0$ hold. Then calculating the second total time derivative $\ddot{\sigma}$ along the trajectories of Eq. (4.9), under the conditions outlined above in Eq. (4.8), we obtain

$$\ddot{\sigma} = h(t,x) + g(t,x)u$$

where the functions $h = \ddot{\sigma}|_{u=0}$, $g = \frac{\partial}{\partial u}\ddot{\sigma} \neq 0$ are some unknown smooth functions. Suppose that the inequalities

$$0 < K_m \leq g \leq K_M,\ |h| \leq C \tag{4.10}$$

hold globally for some $K_m, K_M, C > 0$. Note that, at least locally, Eq. (4.10) is satisfied for any smooth system (4.8) with the well-defined relative degree 2.

Obviously, no continuous feedback controller of the form $u = \varphi(\sigma, \dot{\sigma})$ can solve the stated problem. Indeed, such a control ensuring $\sigma \equiv 0$ has to satisfy the equality $\ddot{\sigma} \equiv 0$ as well, which means that $\varphi(0,0) = -h(t,x)/g(t,x)$, whenever $\sigma = \dot{\sigma} = 0$ holds. The uncertainty in the problem prevents it, since the controller will not be effective for the simple autonomous linear system $\ddot{\sigma} = c + ku$, $K_m \leq k \leq K_M$, $|c| \leq C$, with $\varphi(0,0) \neq -c/k$. In other words, due to the uncertainty, the 2-sliding mode $\sigma = \dot{\sigma} = 0$ needs to be established.

Assume now that Eq. (4.10) holds globally. Then Eqs. (4.8), (4.10) imply the differential inclusion

$$\ddot{\sigma} \in [-C, C] + [K_m, K_M]\,u \tag{4.11}$$

Most 2-sliding controllers may be considered as controllers for Eq. (4.11) steering $\sigma, \dot{\sigma}$ to 0 in (preferably) finite time. Since the inclusion (4.11) does not "remember" the original system (4.9), such controllers are obviously robust with respect to any perturbations preserving (4.10).

Hence, the problem is to find a feedback

$$u = \varphi(\sigma, \dot{\sigma}) \tag{4.12}$$

such that all the trajectories of Eqs. (4.11), (4.12) converge in finite time to the origin $\sigma = \dot{\sigma} = 0$ of the phase plane $\sigma, \dot{\sigma}$. We will now consider a number of the simplest and most popular controllers solving this problem.

4.2.1 Twisting Controller

The twisting controller described below is historically the first 2-sliding controller which was proposed. It is defined by the formula

$$u = -\left(r_1 \text{sign}(\sigma) + r_2 \text{sign}(\dot{\sigma})\right), \quad r_1 > r_2 > 0 \tag{4.13}$$

Theorem 4.1. *Let r_1 and r_2 satisfy the conditions*

$$(r_1 + r_2)K_m - C > (r_1 - r_2)K_M + C, \ (r_1 - r_2)K_m > C \tag{4.14}$$

The controller in Eq. (4.13) guarantees the appearance of a 2-sliding mode $\sigma = \dot{\sigma} = 0$ attracting the trajectories of the sliding variable dynamics (4.11) in finite time.

Proof. It is easy to see that every trajectory of the system crosses the axis $\sigma = 0$ in finite time. Indeed, due to Eqs. (4.13), (4.14) $\text{sign}(\sigma)\ \text{sign}(\ddot{\sigma}) < 0$ and with $\text{sign}(\sigma)$ being constant for a long time, $\sigma\dot{\sigma} < 0$ is established, while the absolute value of $\dot{\sigma}$ tends to infinity. It follows from Eq. (4.14) that with $\sigma \neq 0$

$$\begin{aligned} -[K_M(r_1 + r_2) + C] \leq \ddot{\sigma}\,\text{sign}(\sigma) \leq -[K_M(r_1 + r_2) - C] < 0 \text{ with } \sigma\dot{\sigma} > 0 \\ -[K_M(r_1 - r_2) + C] \leq \ddot{\sigma}\,\text{sign}(\sigma) \leq -[K_M(r_1 - r_2) - C] < 0 \text{ with } \sigma\dot{\sigma} < 0 \end{aligned} \tag{4.15}$$

According to the Filippov definitions, the values taken on a set of the measure 0 (in particular on any curve) do not matter. Let $\dot{\sigma}_0, \sigma_M, \dot{\sigma}_M$ (Fig. 4.3.) be the trajectory of differential equation

$$\ddot{\sigma} = \begin{cases} -[K_m(r_1 + r_2) - C]\text{sign}(\sigma) & \text{with } \dot{\sigma}\sigma > 0 \\ -[K_M(r_1 - r_2) + C]\text{sign}(\sigma) & \text{with } \dot{\sigma}\sigma \leq 0, \end{cases} \tag{4.16}$$

with the same initial conditions. Assume now for simplicity that the initial values are $\sigma = 0$, $\dot{\sigma} = \dot{\sigma}_0 > 0$ at $t = 0$. Thus, the trajectory enters the half-plane $\dot{\sigma} > 0$. Simple calculation shows that with $\sigma > 0$ the solution of Eq. (4.16) is determined by the equalities

$$\begin{aligned} \sigma &= \sigma_M - \frac{\dot{\sigma}^2}{2[K_m(r_1+r_2)-C]} \ \text{ with } \dot{\sigma} > 0 \\ \sigma &= \sigma_M - \frac{\dot{\sigma}^2}{2[K_M(r_1-r_2)+C]} \text{ with } \dot{\sigma} \leq 0 \end{aligned} \tag{4.17}$$

where σ_M is determined from the equation

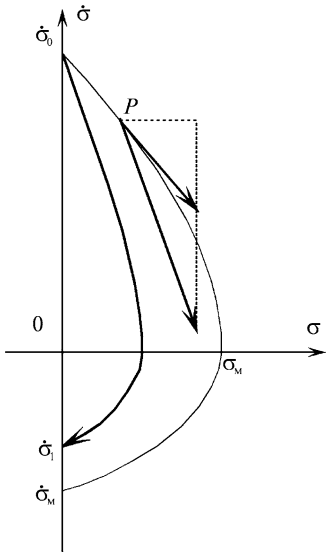

Fig. 4.3 Construction of a majorant trajectory for the twisting controller

$$2[K_M(r_1 + r_2) - C]\sigma_M = \dot{\sigma}_0^2 \tag{4.18}$$

Consider any point $P(\sigma_P, \dot{\sigma}_P)$ of this curve (Fig. 4.3). The velocity of Eqs. (4.11), (4.13) at this point has coordinates $(\dot{\sigma}_P, \ddot{\sigma}_P)$. Hence, the horizontal component of the velocity depends only on the point itself. Since the vertical component satisfies the inequalities (4.15), the velocity of Eqs. (4.11), (4.13) always "looks" into the region bounded by the axis $\sigma = 0$ and curve (4.17). That curve is called the majorant. Let the trajectory of Eqs. (4.11), (4.13) next intersect the axis $\sigma = 0$ at the point $\dot{\sigma}_1$. Then, obviously, $|\dot{\sigma}_1| \leq |\dot{\sigma}_M|$ and

$$|\dot{\sigma}_1| / |\dot{\sigma}_0| \leq [K_M(r_1 - r_2) + C] / [K_M(r_1 + r_2) - C]^{1/2} = q < 1 \tag{4.19}$$

Extending the trajectory into the half-plane $\sigma < 0$, after similar reasoning, guarantees that the successive crossings of the axis $\sigma = 0$ satisfy the inequality

$$|\dot{\sigma}_{i+1}| / |\dot{\sigma}_i| \leq q < 1 \tag{4.20}$$

as shown in (Fig. 4.3). Therefore, the algorithm obviously converges. Next the convergence time is to be estimated. The real trajectory consists of an infinite number of segments belonging to the half-planes $\sigma \geq 0$ and $\sigma \leq 0$ (Fig. 4.4). On each of these segments $\dot{\sigma}$ changes monotonously according to Eq. (4.15). The total variance of the function $\dot{\sigma}(t)$ is

$$Var(\dot{\sigma}(\cdot)) = |\dot{\sigma}_{i+1}| \leq |\dot{\sigma}_0| \left(1 + q + q^2 + \ldots\right) = \frac{|\dot{\sigma}_0|}{1 - q} \tag{4.21}$$

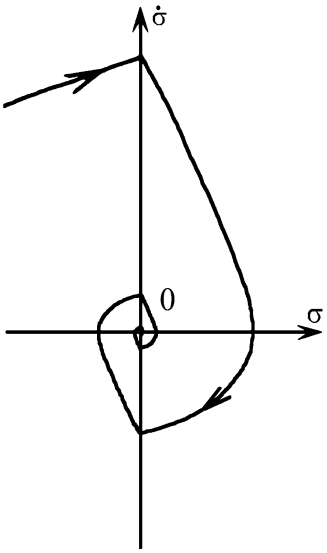

Fig. 4.4 Twisting controller trajectory

and the total convergence time is estimated as

$$T \leq \sum \frac{|\dot{\sigma}_i|}{[K_m(r_1 - r_2) - C]} \leq \frac{|\dot{\sigma}_0|}{(1-q)[K_m(r_1 - r_2) - C]} \tag{4.22}$$

The proof of the theorem is complete. □

Remark 4.2. Note that considering the successive intersections of the trajectory with the σ axis, a similar inequality can be obtained:

$$|\sigma_{i+1}| \,/\, |\sigma_i| \leq [K_M\,(r_1 - r_2) + C] \,/\, [K_M\,(r_1 + r_2) - C]^{1/2} = q^2 < 1 \tag{4.23}$$

which also can be used for the proof. The same majorant curves are used, taken in the half-plane $\dot{\sigma} \leq 0$ or $\dot{\sigma} \geq 0$.

Remark 4.3. In practice the parameters are *never* assigned according to inequalities (4.14). Usually the real system is not exactly known, the model itself is not really adequate, and the estimations of parameters K_M, K_m, C are much larger than the actual values (often 100 times larger!). The larger the controller parameters, the more sensitive is the controller to any switching imperfections and measurement noises. Thus, a pragmatic way is to adjust the controller parameters via computer simulations. (In fact this is true with respect to all controllers described in this chapter.)

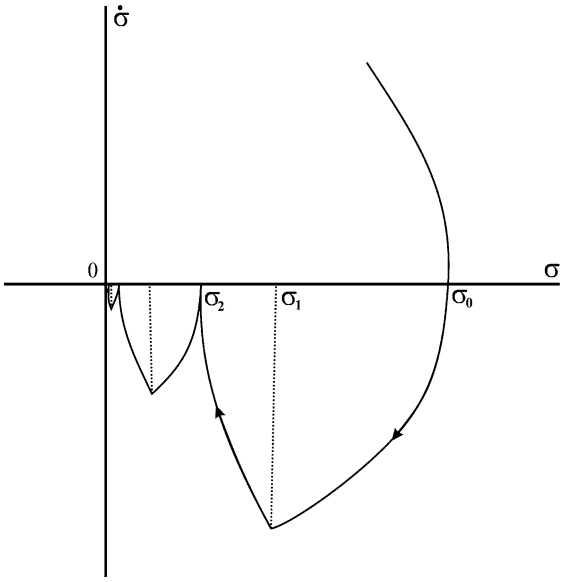

Fig. 4.5 Suboptimal controller trajectory convergence (the case of $q < 1$)

4.2.2 Suboptimal Algorithm

The so-called suboptimal controller is given by

$$u = -r_1 \text{sign}\left(\sigma - \sigma^*/2\right) + r_2 \text{sign}\left(\sigma^*\right), \quad r_1 > r_2 > 0, \tag{4.24}$$

where

$$r_1 - r_2 > \frac{C}{K_m}, \quad r_1 + r_2 > \frac{4C + K_M(r_1 - r_2)}{3K_m}, \tag{4.25}$$

and σ^* is the value of σ detected at the last time when $\dot{\sigma}$ was equal to 0. The initial value of σ^* is equal to 0. Any computer implementation of this controller requires successive measurements of $\dot{\sigma}$ or σ. Usually, the detection $\dot{\sigma} = 0$ occurs when the difference between successive measurements of $\Delta\sigma$ changes sign. The idea of the controller is directly derived from time-optimal control of a double integrator. A trajectory of the suboptimal controller is shown in the coordinates σ,$\dot{\sigma}$ in Fig. 4.5.

In the figure σ_0, σ_2 are two successive points of the intersection with the axis $\dot{\sigma} = 0$ and $\sigma_1 = \sigma_0/2$. Similar to the proof of the twisting controller inequality (4.19), this implies that

$$|\sigma_1 - \sigma_2| \,/\, |\sigma_0 - \sigma_1| \leq [K_M\,(r_1 - r_2) + C] \,/\, [K_M\,(r_1 + r_2) - C] = q^2 < 2 \tag{4.26}$$

(see the remark after the twisting controller proof). Let $\sigma_0 > 0$, then considering the cases $\sigma_2 > 0$ and $\sigma_2 \leq 0$ one can obtain that $|\sigma_2| \,/\, |\sigma_0| \leq 1/2$, which also provides finite-time convergence. Note that with $q < 1$ the overshoot case $\sigma_2 \leq 0$ is excluded and monotonic convergence to zero is ensured (Fig. 4.5). The previous results can be summarized as the following theorem:

Theorem 4.2. *Controller* (4.24), (4.25) *guarantees the finite-time establishment and keeping of the 2-sliding mode* $\sigma \equiv 0$ *for the sliding variable dynamics satisfying* (4.11).

□

4.2.3 Control Algorithm with Prescribed Convergence Law

The controller with prescribed convergence law is defined as

$$u = -\alpha \ \mathrm{sign}\left(\dot{\sigma} + \xi(\sigma)\right), \ \alpha > 0 \tag{4.27}$$

where $\xi(\sigma)$ is a continuous function smooth everywhere except $\sigma = 0$. It is assumed that all solutions of the differential equation $\dot{\sigma} + \xi(\sigma) = 0$ converge to 0 in finite time. The idea is to keep $\dot{\sigma} + \xi(\sigma) = 0$ in the 1-sliding mode.
Choosing $\xi(\sigma) = \beta|\sigma|^{1/2} \mathrm{sign}\,\sigma$, $\beta > 0$, in Eq. (4.27) yields the controller

$$u = -\alpha \ \mathrm{sign}(\dot{\sigma} + \beta|\sigma|^{1/2} \mathrm{sign}\,\sigma) \tag{4.28}$$

The following result can be proved:

Theorem 4.3. *Controller* (4.28) *guarantees the establishment and maintenance of a 2-sliding mode* $\sigma \equiv 0$ *for the sliding variable dynamics given by Eq.* (4.11), *in finite time.*

Proof. Differentiating the function $\Sigma = \dot{\sigma} + \beta\,|\sigma|^{1/2} \mathrm{sign}\,(\sigma)$ along the trajectory yields

$$\dot{\Sigma} \in [-C, C] - \alpha\,[K_m, K_M] \,\mathrm{sign}\,(\Sigma) + \tfrac{1}{2}\beta\dot{\sigma}\,|\sigma|^{-1/2} \tag{4.29}$$

Checking the condition $\dot{\Sigma}\,\mathrm{sign}(\Sigma) < const < 0$ in a vicinity of each point on the curve $\Sigma = 0$, using $\dot{\sigma} = -\beta\,|\sigma|^{1/2} \mathrm{sign}\,(\sigma)$, implies that the 1-sliding-mode existence condition holds at each point except at the origin, if $\alpha K_m - C > \beta^2/2$.

The trajectories of the inclusion inevitably hit the curve $\Sigma = 0$ due to geometrical reasons. Indeed, each trajectory, starting with $\Sigma > 0$, terminates sooner or later at the semi-axis $\sigma = 0, \dot{\sigma} < 0$, if $u = -\alpha \cdot \mathrm{sign}(\Sigma)$ keeps its constant value $-\alpha$ (Fig. 4.6). Thus, on the way it inevitably hits the curve $\Sigma = 0$. The same is true for the trajectory starting with $\Sigma < 0$. From that moment the trajectory slides along the curve $\Sigma = 0$ towards the origin and reaches it in finite time. Obviously, each trajectory starting from a disk centered at the origin comes to the origin in a finite time, the convergence time being uniformly bounded in the disk.

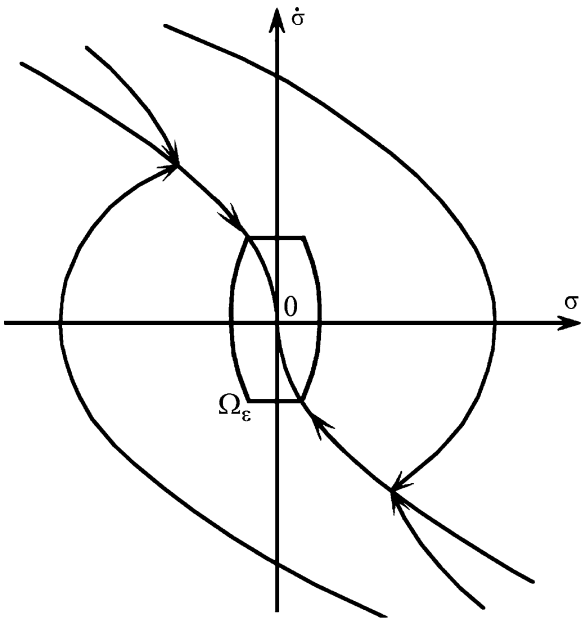

Fig. 4.6 Trajectories of the controller with the prescribed convergence law

Consider the region Ω_ε confined by the lines $\dot{\sigma} = \pm\varepsilon$ and the trajectories of the differential equations $\ddot{\sigma} = -C + K_m\alpha$ with initial conditions $\sigma = \varepsilon^2/\beta^2$, $\dot{\sigma} = \varepsilon$, and $\ddot{\sigma} = C - K_m\alpha$ with initial conditions $\sigma = -\varepsilon^2/\beta^2$, $\dot{\sigma} = \varepsilon$ (Fig. 4.6). No trajectory starting from the origin can leave Ω_ε. Since ε can be taken arbitrarily small, the trajectory cannot leave the origin. This completes the proof. □

4.2.4 Quasi-Continuous Control Algorithm

An important class of controllers comprises the recently proposed so-called *quasi-continuous* controllers, featuring control continuous everywhere except the 2-sliding manifold $\sigma = \dot{\sigma} = 0$ itself. Since the 2-sliding condition requires the simultaneous fulfillment of two exact equalities, in the presence of any small noises and disturbances, the general-case trajectory does not ever hit the 2-sliding set. Hence, in practice the condition $\sigma = \dot{\sigma} = 0$ is never fulfilled, and the control remains continuous function of time, all the time. The larger the noises and switching imperfections, the worse the accuracy and the slower the changing rate of u. As a result, chattering is significantly reduced. The following is a 2-sliding controller with such features:

$$u = -\alpha \frac{\dot{\sigma} + \beta|\sigma|^{1/2}\text{sign}(\sigma)}{|\dot{\sigma}| + \beta|\sigma|^{1/2}} \tag{4.30}$$

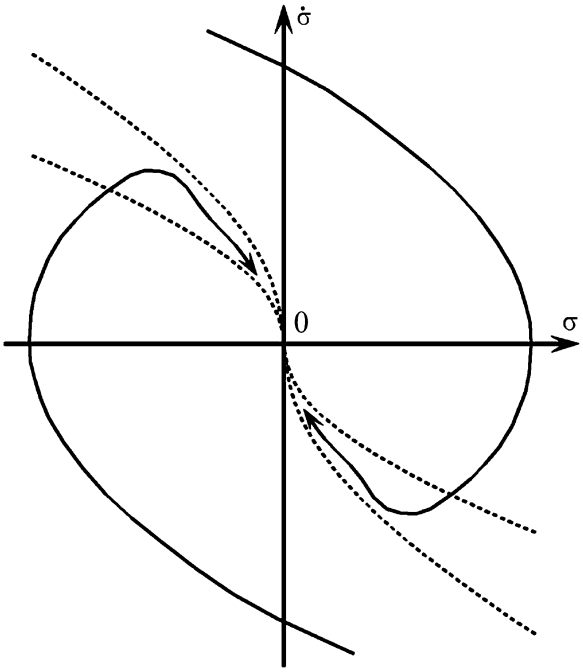

Fig. 4.7 Trajectories of the quasi-continuous controller

This control is continuous everywhere except the origin and it vanishes on the parabola $\dot{\sigma} + \beta\ |\sigma|^{1/2}\ \mathrm{sign}\,(\sigma) = 0$. For sufficiently large α, there are numbers $\rho_1, \rho_2 : 0 < \rho_1 < \beta < \rho_2$ such that all the trajectories enter the region between the curves $\dot{\sigma} + \rho_i\ |\sigma|^{1/2}\ \mathrm{sign}\,(\sigma) = 0,\ i = 1, 2$ and cannot leave it (Fig. 4.7).

Theorem 4.4. *Let*

$$\alpha, \beta > 0,\ \alpha K_m - C > 0 \tag{4.31}$$

and suppose the inequality

$$\alpha K_m - C - 2\alpha K_m \frac{\beta}{\rho + \beta} - \frac{1}{2}\rho^2 > 0 \tag{4.32}$$

holds for some positive $\rho > \beta$ (it is always true for a sufficiently large α), then the controller (4.30) guarantees the establishment of a stable 2-sliding mode $\sigma \equiv 0$ for the sliding variable dynamics given by Eq. (4.11), in finite time.

Remark 4.4. The conditions of the theorem can be solved for α, but the resulting expressions are redundantly cumbersome.

Proof. Denote $\rho = -\dot{\sigma} / |\sigma|^{1/2}$. Due to the symmetry of the problem, it is enough to consider the case of $\sigma > 0$ and $-\infty < \rho < \infty$. Calculations show that $u = \alpha\,(\rho - \beta)\,/\,(|\rho| + \beta)$ and

$$\dot{\rho} \in \left([-C, C] - [K_m, K_M]\, \alpha \frac{\rho - \beta}{|\rho| + \beta} + \frac{1}{2}\rho^2 \text{sign}\,(\sigma) \right) |\sigma|^{-1/2} \tag{4.33}$$

With a negative or small positive ρ, the rotation velocity $\dot{\rho}$ is always positive due to Eq. (4.31). Thus there is a positive $\rho_1 < \beta$ such that the trajectories enter the region $\rho > \rho_1$. It is now necessary to show that there is a $\rho_2 > \beta$ such that in some vicinity of $\rho = \rho_2$ the inequality $\dot{\rho} < 0$ holds. This is exactly condition (4.32). Thus, conditions (4.31), (4.32) provide for the establishment and keeping of the inequality $\rho_1 < \rho < \rho_2$ and the proof of the theorem is complete. □

4.2.5 Accuracy of 2-Sliding Mode Controllers

Consider the cases of noisy and/or discrete measurements with respect to the sampling interval τ. We will see in Chap. 6 that the discrete-sampling versions based on the Euler scheme provide an accuracy level of $\sigma = O(\tau^2)$, $\dot{\sigma} = O(\tau)$ in the absence of noise. Noisy measurements lead to the accuracy $\sigma = O(\varepsilon)$, $\dot{\sigma} = O(\varepsilon^{1/2})$, if the maximal errors of σ and $\dot{\sigma}$ and the sampling are of the order of ε and $\varepsilon^{1/2}$, respectively, and the maximal sampling interval τ is of the order $\varepsilon^{1/2}$. Note that this result does not require any practical dependence between τ and noise magnitudes. Indeed, in practice there are always specific values of noise magnitudes and sampling intervals, which can always be considered as a sample of an infinite family (in a nonunique way). Moreover, one can always reduce either the noise magnitudes or the sampling interval, preserving the same upper accuracy estimation.

4.3 Control of Relative Degree One Systems

All the controllers described this far require real-time measurements of $\dot{\sigma}$ or at least of sign($\dot{\sigma}$). In other words, in order to guarantee $\sigma = \dot{\sigma} = 0$, both σ and $\dot{\sigma}$ measurements are needed. This is reasonable but, nevertheless, not inevitable. The following controller can be used instead of the conventional (first-order) sliding mode using the same available information.

4.3.1 Super-Twisting Controller

Consider once more the dynamical system (4.9) of relative degree 1 and suppose that

$$\dot{\sigma} = h(t, x) + g(t, x)u \tag{4.34}$$

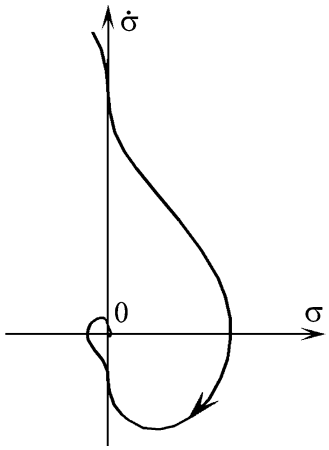

Fig. 4.8 Trajectory of the super-twisting controller

Furthermore assume that for some positive constants C, K_M, K_m, U_M, q

$$|\dot{h}| + U_M|\dot{g}| \leq C, \quad 0 \leq K_m \leq g(t, x) \leq K_M, \quad |h/g| < qU_M, \quad 0 < q < 1 \tag{4.35}$$

hold and define

$$u = -\lambda|\sigma|^{1/2}\text{sign}(\sigma) + u_1, \quad \dot{u}_1 = \begin{cases} -u, & |u| > U_M \\ -\alpha\text{sign}(\sigma), & |u| \leq U_M \end{cases} \tag{4.36}$$

Then the following result is obtained.

Theorem 4.5. *With $K_m\alpha > C$ and λ sufficiently large, the controller (4.36) guarantees the appearance of a 2-sliding mode $\sigma = \dot{\sigma} = 0$ in system (4.34), which attracts the trajectories in finite time. The control u enters in finite time the segment $[-U_M, U_m]$ and stays there. It never leaves the segment, if the initial value is inside at the beginning.*

Remark 4.5. Note that the controller does not need measurements of $\dot{\sigma}$.

The controller given in Eq. (4.36) is called the super-twisting controller. The corresponding phase portrait is shown in Fig. 4.8. A sufficient (*very crude!*) condition for validity of the theorem is

$$\lambda > \sqrt{\frac{2}{(K_m\alpha - C)}}\frac{(K_m\alpha + C)K_M(1+q)}{K_m^2(1-q)} \tag{4.37}$$

Proof. Computing $\dot{u}$ with $|u| > U_M$ yields $\dot{u} = -\frac{1}{2}\lambda\dot{\sigma}|\sigma|^{-1/2} - u$. It follows from Eqs. (4.34), (4.35) that $\dot{\sigma}u > 0$ with $|u| > U_M$ and thus, $\dot{u}u < 0$, and u moves

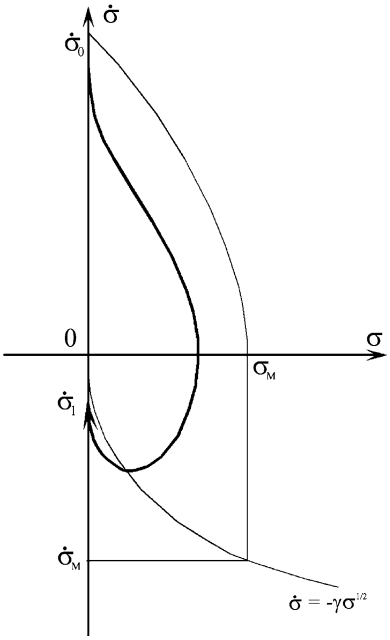

Fig. 4.9 A majoring curve for the super-twisting controller

towards the segment $|u| \leq U_M$. Therefore $|u| \leq U_M$ is established in finite time, for $|\dot{u}| > U_M$ when $|u| > U_M$. Note that a 1-sliding mode with $u = -U_m \text{sign}(\sigma)$ could exist during time intervals of constant $\text{sign}(\sigma)$ (e.g., see Fig. 4.1). The following equation is satisfied with $|u| < U_M$, $\sigma \neq 0$:

$$\ddot{\sigma} = \dot{h} + \dot{g}u - g\frac{1}{2}\lambda\frac{\dot{\sigma}}{|\sigma|^{1/2}} - g\,\alpha\,\text{sign}(\sigma)$$

The trivial identity $\frac{d}{dt}|\sigma| = \dot{\sigma}\text{sign}(\sigma)$ is used here. Note that once more, the values taken on sets of measure 0 are not accounted for; thus the differentiation is performed with $\text{sign}(\sigma) = const$. The latter equation may be rewritten as

$$\ddot{\sigma} \in [-C, C] - [K_m, K_M]\left(\frac{1}{2}\lambda\frac{|\dot{\sigma}|}{|\sigma|^{1/2}} + \alpha\text{sign}\,(\sigma)\right) \tag{4.38}$$

This inclusion does not 'remember' anything about the original system. Then similarly to the proof of Theorem 4.1, with $\sigma > 0$, $\dot{\sigma} > 0$, the real trajectory is confined by the axes $\sigma = 0, \dot{\sigma} = 0$ and the trajectory of the equation $\ddot{\sigma} = -(K_m\alpha - C)$. Let σ_M be the intersection of this curve with axis $\dot{\sigma} = 0$. Obviously, $2(K_m\alpha - C)\sigma_M = \dot{\sigma}_0^2$ (Fig. 4.9). It is easy to see from Fig. 4.9 that

$$\sigma > 0, \quad \dot{\sigma} > 0, \quad \frac{1}{2}\lambda\frac{|\dot{\sigma}|}{|\sigma|^{1/2}} > \frac{C}{K_m} + \alpha \quad \Rightarrow \quad \ddot{\sigma} > 0$$

Thus, the majoring curve with $\sigma > 0$ is constructed from the following curves (Fig. 4.9):

$$\dot{\sigma}^2 = 2\,(K_m\alpha - C)\,(\sigma_M - \sigma) \;\text{ with } \dot{\sigma} > 0,\; \dot{\sigma}_0^2 = 2\,(K_m\alpha - C)\,\sigma_M$$

$$\sigma = \sigma_M \;\text{ with } 0 \geq \dot{\sigma} \geq -\frac{2}{\lambda}\left(\frac{C}{K_m} + \alpha\right)\sigma^{1/2}$$

$$\dot{\sigma} = \dot{\sigma}_M = -\frac{2}{\lambda}\left(\frac{C}{K_m} + \alpha\right)\sigma_M^{1/2} \text{ with } 0 \leq \sigma \leq \sigma_M$$

The condition $|\dot{\sigma}_M/\dot{\sigma}_0| < 1$ is sufficient for the algorithm convergence while $|u| < U_M$. That condition is rewritten as

$$\frac{2(K_m\alpha + C)^2}{\lambda^2 K_m^2(K_m\alpha - C)} < 1$$

Unfortunately, the latter inequality is still not sufficient, for this consideration does not include the possible 1-sliding mode keeping of $u = \pm U_M$. It is easy to see that such a mode is not possible with $\sigma\dot{\sigma} > 0$. Indeed, in that case $u\dot{\sigma}$ stays negative and does not allow any sign switching of $u - U_m$. On the other hand, from Eqs. (4.34), (4.35) and $|u| \leq U_M$, in such a sliding mode

$$K_m(1-q)U_M \leq |\dot{\sigma}| = g\,|h/g + u| \leq K_M(1+q)U_M$$

Thus, $\dot{\sigma}_0 \leq K_M(1+q)U_M$, and the condition

$$\left|\frac{\dot{\sigma}_M}{\dot{\sigma}_0}\right| < \frac{K_m(1-q)U_M}{K_M(1+q)U_M} = \frac{K_m(1-q)}{K_M(1+q)}$$

is sufficient to avoid keeping $u = \pm U_M$ in sliding mode. The resulting condition above coincides with Eq. (4.37).

It is now required to prove the finite-time convergence. It is enough to consider only a sufficiently small vicinity of the origin, where $|u| < U_M$ is guaranteed. Consider an auxiliary variable $\xi = h(t,x) + g(t,x)u_1$. Obviously, $\xi = \dot{\sigma}$ at the moments when $\sigma = 0$, and $u_1 \to -h/g$ as $t \to \infty$. Thus, $\xi = g(h/g + u_1)$ tends to zero. Starting from the moment when $|u_1| < U_M$ holds, its derivative $\dot{\xi} = \dot{h} + \dot{g}u_1 - g\,\alpha\,\mathrm{sign}(x)$ satisfies the inequalities

$$0 < K_m\alpha - C \leq -\dot{\xi}\,\mathrm{sign}(\sigma) \leq K_M\alpha + C$$

As in the proof of Theorem 4.1, the total variation of ξ is equal to $\sum |\dot{\sigma}_i|$, is bounded by a geometric series, and therefore converges. The total convergence time $T \leq \sum |\dot{\sigma}_i|/(K_m\alpha - C)$ and the proof of the theorem is complete. □

Note that the accuracy estimations formulated at the end of Sect. 4.2 remain valid for sufficiently small noises and/or sampling intervals. This robustness feature leads to the application of the controller in observation and identification. One of the most important applications is considered in the next Subsection.

4.3.2 First-Order Differentiator

The super-twisting controller is used for systems of relative degree 1. In other words it can be used instead of a standard 1-sliding-mode controller in order to avoid chattering. However for relative degree 2 systems a 2-sliding controller, like a twisting one, is needed to stabilize system (4.6) in finite time. In order to avoid the use of $\dot{\sigma}$ measurements, a differentiator (observer) is needed. Popular linear high-gain observers cannot fulfill this task because they only provide asymptotic stabilization at an equilibrium state. The differentiator needed here has to feature robust exact differentiation with finite-time convergence in the absence of the measurement noise.

Let the input signal $f(t)$ be a function defined on $[0, \infty)$ consisting of a bounded Lebesgue-measurable noise with unknown features and an unknown base signal $f_0(t)$ with the first derivative having a known global Lipschitz constant $L > 0$. The problem is to find real-time robust estimations of $f_0(t)$ and $\dot{f}_0(t)$ which are exact in the absence of measurement noise.

Consider the auxiliary system $\dot{z}_0 = v$, where v is a control input. Let $\sigma_0 = z_0 - f_0(t)$ and let the task be to keep $\sigma_0 = 0$ in a 2-sliding mode. In that case $\sigma_0 = \dot{\sigma}_0 = 0$, which means that $z_0 = f_0(t)$ and $\dot{f}_0 = v$. The system can be rewritten as

$$\dot{\sigma}_0 = -\dot{f}_0(t) + v, \quad |\ddot{f}_0| \le L$$

The function $\dot{f}_0$ can be not smooth, but its derivative $\ddot{f}_0$ exists almost everywhere due to the Lipschitz property of $\dot{f}_0$. A modification of the super-twisting controller

$$\begin{aligned} v &= -\lambda_1 |\sigma_0|^{1/2} \mathrm{sign}(\sigma_0) + z_1 \\ \dot{z}_1 &= -\lambda_2 \mathrm{sign}(\sigma_0) \end{aligned}$$

is applied here. The modification is needed, for neither $\dot{f}_0(t)$ nor v is bounded. The resulting form of the differentiator is

$$\begin{aligned} \dot{z}_0 &= v = -\lambda_1 \left| z_0 - f(t) \right|^{1/2} \mathrm{sign}\left(z_0 - f(t) \right) + z_1 \\ \dot{z}_1 &= -\lambda_0 \mathrm{sign}(z_0 - f(t)) \end{aligned} \tag{4.39}$$

where both v and z_1 can be taken as the differentiator outputs.

Theorem 4.6. *In the absence of noise for any $\lambda_0 > L$ for every sufficiently large λ_1, both v and z_1 converge in finite time to $\dot{f}_0(t)$, while z_0 converges to $f_0(t)$.*

The proof of the theorem is actually contained in the proof of Theorem 4.5. Sufficient crude convergence conditions are

$$\lambda_0 > L, \quad \frac{2(\lambda_0 + L)^2}{\lambda_1^2 (\lambda_0 - L)} < 1 \tag{4.40}$$

Theorem 4.7. *Let the input noise satisfy the inequality* $|f(t) - f_0(t)| \le \varepsilon$. *Then the following inequalities are established in finite time for some positive constants* μ_1, μ_2, μ_3, *depending exclusively on the parameters of the differentiator and* L:

$$|z_0 - f_0(t)| \le \mu_1 \varepsilon, \quad |z_1 - \dot{f}_0(t)| \le \mu_2 \varepsilon^{1/2}, \quad |v - \dot{f}_0(t)| \le \mu_3 \varepsilon^{1/2}$$

Moreover, these asymptotics cannot be improved.

Sketch of the proof. Let $\sigma_0 = z_0 - f_0(t)$, $\sigma_1 = z_1 - \dot{f}_0(t)$, then

$$\dot{\sigma}_1 = -\ddot{f}_0(t) - \lambda_0 \text{sign}(\sigma_0) \in [-L,\ L] - \lambda_0 \text{sign}(\sigma_0),$$

and the differentiator equations in the absence of the input noise may be replaced by the inclusion

$$\begin{aligned} \dot{\sigma}_0 &= -\lambda_1 |\sigma_0|^{1/2} \text{sign}(\sigma_0) + \sigma_1 \\ \dot{\sigma}_1 &\in -[\lambda_0 - L,\ \lambda_0 + L] \text{sign}(\sigma_0) \end{aligned} \tag{4.41}$$

Its solutions converge to the origin $\sigma_0 = 0$, $\sigma_1 = 0$ in finite time. With $\varepsilon \neq 0$ inclusion (4.41) turns into

$$\begin{aligned} \dot{\sigma}_0 &\in -\lambda_1 |\sigma_0 + [-\varepsilon,\ \varepsilon]|^{1/2} \text{sign}(\sigma_0 + [-\varepsilon,\ \varepsilon]) + \sigma_1 \\ \dot{\sigma}_1 &\in -[\lambda_0 - L,\ \lambda_0 + L] \text{sign}(\sigma_0 + [-\varepsilon,\ \varepsilon]) \end{aligned}$$

For small $\varepsilon = \varepsilon_0$, the trajectories are concentrated in a small set $\sigma_0 \le \kappa_0$, $\sigma_1 \le \kappa_1$ and stay there forever. Apply a combined transformation of coordinates, time, and parameters:

$$G_\nu \ : (\sigma_0,\ \sigma_1,\ t,\ \varepsilon_0) \mapsto (\nu^2 \sigma_0,\ \nu \sigma_1,\ \nu t,\ \nu^2 \varepsilon_0)$$

Then it is easy to see that the trajectories of inclusion (4.40) are transferred into the trajectories of the same inclusion, but with different noise magnitude $\varepsilon = \nu^2 \varepsilon_0$. Now define $\nu = \sqrt{\varepsilon / \varepsilon_0}$ and get that the new attracting invariant set satisfies the inequalities $\sigma_0 \le \nu^2 \kappa_0 = (\kappa_0 / \varepsilon_0)\varepsilon$, $\xi \le \nu \kappa_1 = (\kappa_1 / \sqrt{\varepsilon_0})\varepsilon$. □

Theorem 4.8. *Let parameters* $\lambda_1 = \Lambda_1$, $\lambda_0 = \Lambda_0$ *of the differentiator in Eqs.* (4.39), (4.40) *guarantee exact differentiation with* $L = 1$. *Then parameters* $\lambda_1 = \Lambda_1 L^{1/2}$, $\lambda_0 = \Lambda_0 L$ *are valid for any* $L > 0$ *and guarantee the accuracy level*

$$|z_0 - f_0(t)| \le \mu_1 \varepsilon, \quad |z_1 - \dot{f}_0(t)| \le \mu_2 L^{1/2} \varepsilon^{1/2}, \quad |v - \dot{f}_0(t)| \le \mu_3 L^{1/2} \varepsilon^{1/2}$$

for some positive constants μ_1, μ_2, μ_3.

Proof. Denote $\tilde{f} = f/L$, then the following differentiator provides for the exact differentiation of $\tilde{f}(t)$:

$$\begin{aligned} \dot{\tilde{z}}_0 &= -\Lambda_1 |\tilde{z}_0 - \tilde{f}(t)|^{1/2} \text{sign}(\tilde{z}_0 - \tilde{f}(t)) + \tilde{z}_1 \\ \dot{\tilde{z}}_1 &= -\Lambda_0 \text{sign}(\tilde{z}_1 - \tilde{f}(t)) \end{aligned}$$

By multiplying by L and defining $z_0 = L\tilde{z}_0$, $z_1 = L\tilde{z}_1$, the statement of the theorem is proven. □

The parameter choices $\lambda_1 = 1.5L^{1/2}$, $\lambda_0 = 1.1L$ and $\lambda_1 = L^{1/2}$, $\lambda_0 = 2L$ are valid, even though they do not satisfy (4.40). The first one of these choices seems to be a good compromise providing a reasonably fast convergence and high accuracy.

Remark 4.6. Note that while v is noisy in the presence of the input noise, z_1 is a Lipschitzian signal, but small input noises lead to a small phase delay of z_1.

Example 4.1. Suppose that $t_0 = 0$, the initial values of the internal variable $z_0(0)$ and the "measured" input signal $f(0)$ coincide, and the initial value of the output signal z_1 is zero. The simulation was carried out using the Euler method with measurement and integration steps equaling 10^{-4}.

The proposed differentiator (4.39), (4.40) was compared with a simple linear differentiator described by the transfer function $\frac{s}{(0.1s+1)^2}$. Such a differentiator is actually a combination of the ideal differentiator and a low-pass filter. The differentiator parameters were chosen as $\lambda_1 = 6$, $\lambda_0 = 8$. The output signals $f(t) = \sin(t) + 5t$, $f(t) = \sin(t) + 5t + 0.01\cos(10t)$, and $f(t) = \sin(t) + 5t + 0.001\cos(30t)$ together with the ideal derivatives $\dot{f}_0(t)$ are shown in Fig. 4.10. The linear differentiator is seen not to differentiate exactly. At the same time it is highly insensitive to any signals with frequency above 30. The proposed differentiator handles properly any input signal f with $|\ddot{f}| \leq 7$ regardless the signal spectrum.

4.4 Differentiator-Based Output-Feedback 2-SM Control

We are now able to construct a robust output-feedback 2-sliding mode (2-SM) controller for the system with relative degree 2. Recall that the system is described by the equation and conditions

$$\dot{x} = a(t,x) + b(t,x)u$$
$$0 < K_m \leq \frac{\partial}{\partial u}\ddot{\sigma} \leq K_M, \ |\ddot{\sigma}| \leq C$$

The control is to solve the stabilization problem in finite time, only using measurements of σ. The robust exact differentiation of σ is always possible due to the boundedness of $\ddot{\sigma} \in [-C, C] + [K_m, K_M u]$ with bounded control u. Combining any above 2-sliding controller $u = -U(\sigma, \dot{\sigma})$ and the differentiator achieves

$$\begin{aligned} u &= -U(\sigma, z_1) \\ \dot{z} &= -\lambda_1 |z - \sigma|^{1/2} \mathrm{sign}(z - \sigma) + z_1, \\ \dot{z}_1 &= -\lambda_2 \mathrm{sign}(z - \sigma), \ \ \lambda_1 = 1.5L^{1/2}, \ \lambda_2 = 1.1L \end{aligned} \tag{4.42}$$

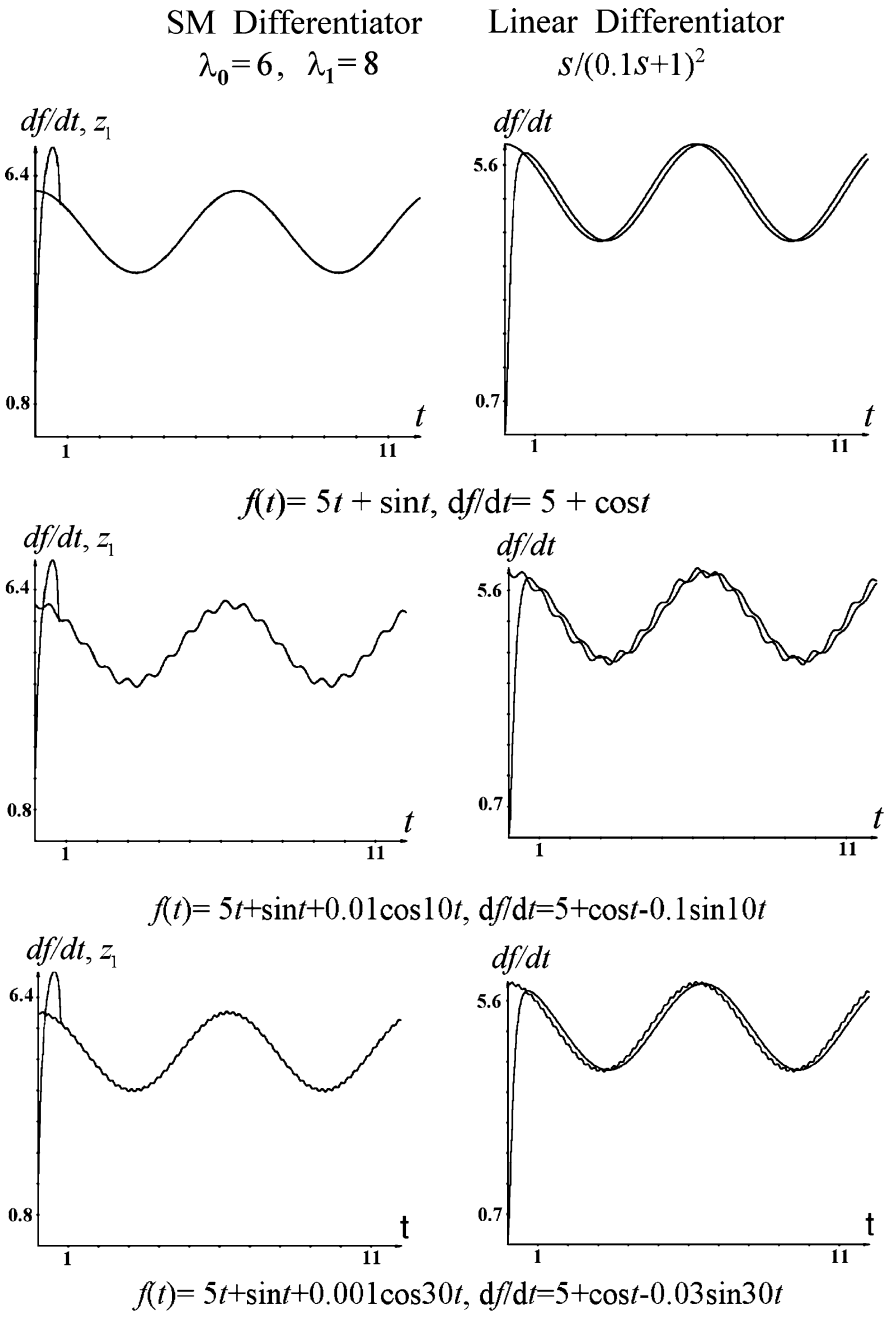

Fig. 4.10 Comparison of the 2-sliding mode-based differentiator and a linear filter

Any value $L > C + K_M \sup |U|$ can be used here. As a consequence of Theorem 4.1 and Theorem 4.6 the controller provides exact stabilization and finite-time convergence. It can be proven that in the presence of a bounded Lebesgue-measurable noise with the maximal magnitude ε, the steady-state accuracies $\sup |\sigma|$ and $\sup|\dot{\sigma}|$ are proportional to ε and $\sqrt{\varepsilon}$, respectively. Note that in practice the differentiator parameter L is often taken conservatively large to provide for the better closed-loop performance in the presence of noises.

Example 4.2. Consider the dynamic system

$$\ddot{x} = \sin(14.12t) + (1.5 + 0.5\cos(21t))u$$
$$\sigma = x,$$

with $C = 1,\ K_m = 1,\ K_M = 2$ and the output-feedback control

$$u = -5\,\mathrm{sign}\, z_0 - 3\,\mathrm{sign}\, z_1$$
$$\dot{z}_0 = -7|z_0 - x|^{1/2}\mathrm{sign}(z_0 - x) + z_1$$
$$\dot{z}_1 = -18\mathrm{sign}(z_0 - x)$$

At the time instant $t = 0$ the initial values $z_0(0) = x(0),\ z_1 = 0$ were taken. The trajectory in the plane $x\dot{x}$ and the mutual graph of x, $\dot{x}$, and z_1 are shown in Fig. 4.11a,b, respectively. The graph of z_0 is not shown, since one cannot distinguish it from x. Convergence in the presence of a high-frequency noise with magnitude 0.01 is shown in Fig. 4.11c,d, respectively. The resulting steady-state accuracies are $|x| \le 0.041$ and $|\dot{x}| \le 0.79$.

4.5 Chattering Attenuation

A problem with conventional (first-order) sliding mode control is attenuation of the chattering effect. However 2-sliding mode control provides effective tools for the reduction or even practical elimination of the chattering, without compromising the benefits of the standard sliding mode. Recalling the problem statement from Sect. 4.3.1, let the relative degree of the system (4.5) be 1, and instead of Eqs. (4.8), (4.10) assume

$$\dot{\sigma} = h(t,x) + g(t,x)u,\ 0 < K_m \le g \le K_M,\ |h| \le C \tag{4.43}$$

where the functions g, h are some unknown smooth functions. Let also the control $u = -k\ \mathrm{sign}\,(\sigma)$ solve the problem of establishing and keeping $\sigma \equiv 0$. In particular, assume that

$$kK_m - C > 0 \tag{4.44}$$

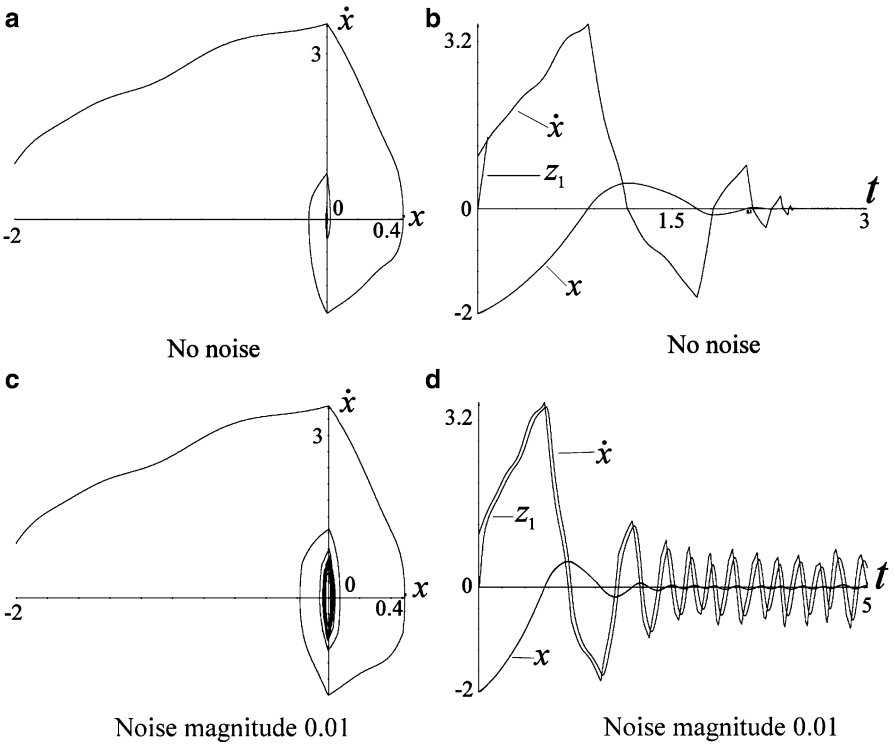

Fig. 4.11 Output-feedback 2-sliding control

Consider $\dot{u}$ as a new virtual control, in order to overcome the chattering. Differentiating (4.43) yields

$$\ddot{\sigma} = h_1(t,x,u) + g(t,x)\dot{u}$$
$$h_1 = h'_t + h'_x\,(a+bu) + \left(g'_t + g'_x\,(a+bu)\right)u$$

Assume that the function $h_1(t,x,u)$ is bounded so that

$$\sup_{|u|\le k_1} |h_1(t,x,u)| = C_1 \tag{4.45}$$

Any previously discussed controller $\dot{u} = U(\alpha,\sigma,\dot{\sigma})$ can be used here in order to overcome the chattering and improve the sliding accuracy of the standard sliding mode. Indeed, define

$$\dot{u} = \begin{cases} -u, |u| > k \\ U(\alpha,\sigma,\dot{\sigma}), |u| \le k \end{cases} \tag{4.46}$$

Theorem 4.9. *Let U be any one of the 2-sliding controllers considered in Sect. 4.2, and suppose the controller parameters are properly chosen in accordance with the corresponding convergence conditions. Then for a sufficiently large parameter α, the controller (4.46) guarantees the establishment of the finite-time stable 2-sliding mode on $\sigma = \dot{\sigma} \equiv 0$.*

Proof. It follows from Eqs. (4.43), (4.44) that the inequality $|\dot{\sigma}| < kK_m - C$ implies $|u| \leq k$. Thus, within the set $|\dot{\sigma}| < kK_m - C$, the system is driven by the controller $\dot{u} = U(\alpha, \sigma, \dot{\sigma})$. Controller(4.46) keeps $|u| \leq k$, and on certain time intervals $u \equiv k$ or $u \equiv -k$ is kept in a 1-sliding mode and the proof of the theorem is complete. □

Lemma 4.1. *Any trajectory of the system (4.43), (4.46) hits in finite time the manifold $\sigma = 0$ or enters the set $\sigma\dot{\sigma} < 0$, $|u| \leq k$.*

Proof. Indeed, suppose that σ does not change its sign. Obviously, the inequality $|u| \leq k$ is established in finite time. If the condition $\sigma\dot{\sigma} < 0$ is attained, the statement of the lemma is true. Suppose that $\sigma\dot{\sigma} \geq 0$ holds, then, according to (4.46), u moves towards $u = -k \operatorname{sign}(\sigma)$ with $|\dot{u}| \geq \min(\alpha, k)$, both if $|u| > k$. or $|u| \leq k$. The conclusion that $u = -k \operatorname{sign}(\sigma)$ can be established only with $\sigma\dot{\sigma} < 0$ proves the lemma. □

Lemma 4.2. *With sufficiently large α any trajectory of the system (4.43), (4.46) hits in finite time the manifold $\sigma = 0$.*

Proof. Denote by S the set defined by the inequalities $|\dot{\sigma}| < kK_m - C$, $\sigma\dot{\sigma} < 0$. There is a specific set Θ for each controller, adjacent to the axis $\sigma = 0$ and lying in the strip S, such that any trajectory entering it either converges in finite time to $\sigma = \dot{\sigma} = 0$ or hits the axis $\sigma = 0$; also no trajectory can enter S outside of Θ. For example, Θ is defined by the inequalities $\left(\dot{\sigma} + \lambda |\sigma|^{1/2} \operatorname{sign}(\sigma)\right)\sigma \leq 0$ and $|\dot{\sigma}| < kK_m - C$ for the controller in Eq. (4.21). Any trajectory starting in S either leaves it in finite time or enters Θ. Thus, there are two options: at some moment on a trajectory that stays out of S, which means that $|\dot{\sigma}| \geq kK_m - C$, $\sigma\dot{\sigma} < 0$, or it enters Θ. In both cases the trajectory hits $\sigma = 0$. The lemma is proven. □

The following lemma is obviously true for any convergent 2-sliding controller.

Lemma 4.3. *There is a vicinity Ω of the origin within the strip $|\dot{\sigma}| < kK_m - C$, which is invariant with respect to the controller $\dot{u} = U(\alpha, \sigma, \dot{\sigma})$.*

Proof. Consider the auxiliary problem when Eq. (4.45) holds independently of the control value and the corresponding differential inclusion. Since all trajectories starting in a closed disk centered at the origin converge to the origin in finite time, the set, which comprises these transient trajectory segments, is an invariant compact for the controller $\dot{u} = U(\alpha, \sigma, \dot{\sigma})$.

All the proposed controllers produce the closed system (4.11) which is invariant with respect to the transformation

$$G_\kappa : (t, \sigma, \dot{\sigma}) \longmapsto \left(\kappa t, \kappa^2\sigma, \kappa\dot{\sigma}\right)$$

Applying now this transformation, the set can be retracted into the strip $|\dot{\sigma}| < kK_m - C$, where Eq. (4.45) is really kept, and the proof of the lemma is complete. □

Lemma 4.4. *For a sufficiently large α, any trajectory starting on the manifold $\sigma = 0$ with $|u| \le k$ enters the invariant set Ω.*

Proof. Any trajectory starting with $\sigma = 0$ and $\dot{\sigma} \neq 0$ inevitably enters the region $\sigma\dot{\sigma} > 0$, $|u| < k$. Within this region $\dot{u} = -\alpha \operatorname{sign}(\sigma)$ holds. Hence, the control u moves towards the value $-k \operatorname{sign}(\sigma)$, and on the way the trajectory hits the set $\dot{\sigma} = 0$, which still features $|u| < k$. From Eq. (4.43), $|u| \le k$ implies the global bound $|\dot{\sigma}| \le kK_M + C$. That restriction is true also at the initial point on the axis $\sigma = 0$. Simple calculations show that the inequality $|\sigma| \le \frac{1}{2}(kK_M + C)^2 / (\alpha K_1 - C_1)$ holds at the moment when $\dot{\sigma}$ vanishes. With sufficiently large α that point inevitably belongs to Ω.

Once the trajectory enters Ω, it continues to converge to the 2-sliding mode according to the corresponding 2-sliding dynamics considered in Sect. 4.2. This proves convergence to the 2-sliding mode. In the presence of small noises and sampling intervals, the resulting motion will take place in a small vicinity of the 2-sliding mode $\sigma = \dot{\sigma} = 0$. Thus, if this motion does not leave Ω, the studied 2-sliding dynamics is still in charge, and the corresponding accuracy estimations remain true. The proof of the lemma is now complete. □

4.6 Case Study: Pendulum Control

Consider a variable-length pendulum control problem where all the motions are restricted to some vertical plane. A load of some known mass m is moving along the pendulum rod (Fig. 4.12).

Its distance from the origin O equals $R(t)$ and is not measured. There is no friction. An engine transmits a torque w that is considered as the control input. The task is to force the angular coordinate x of the rod to follow some profile $x_c(t)$ given in current time. The system is described by the differential equation

$$\ddot{x} = -2\frac{\dot{R}}{R}\dot{x} - g\frac{1}{R}\sin(x) + \frac{1}{mR^2}w \tag{4.47}$$

where $g = 9.81 m/s^2$ is the gravitational constant and the mass m is taken as $m = 1kg$. Let $0 < R_m \le R \le R_M$; also assume that $\dot{R}, \ddot{R}, \dot{x}_c, \ddot{x}_c$ are bounded and $\sigma = x - x_c$ is available. The initial conditions are $x(0) = \dot{x}(0) = 0$. The following functions R and x_c are considered in the simulation:

$$R = 1 + 0.25\sin(4t) + 0.5\cos(t)$$

$$x_c = 0.5\sin(0.5t) + 0.5\cos(t)$$

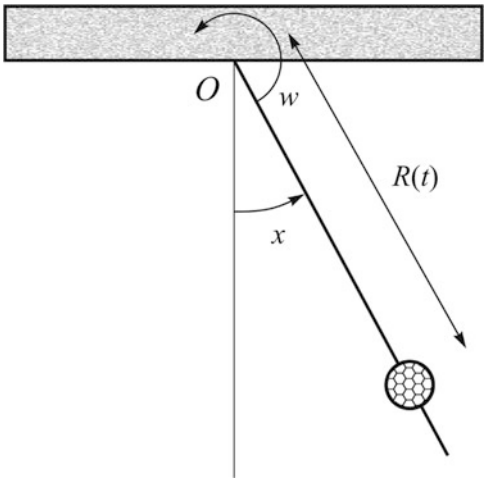

Fig. 4.12 Variable-length pendulum

4.6.1 Discontinuous Control

The relative degree of the system is 2. Here condition (4.10) holds only locally, since $\ddot{\sigma}|_{u=0}$ depends on $\dot{x}$ and is not uniformly bounded. Thus, the controllers are effective only in a bounded vicinity of the origin $x = \dot{x} = w = 0$. The appropriate discontinuous controller, Eq. (4.42) based on a quasi-continuous controller, has the form

$$w = -10\,\frac{z_1 + |\sigma|^{1/2}\mathrm{sign}(\sigma)}{|z_1| + |\sigma|^{1/2}},\ \sigma = x - x_c \tag{4.48}$$

$$\dot{z}_0 = -10.61\ |z_0 - \sigma|^{1/2}\,\mathrm{sign}(z_0 - \sigma) + z_1 \tag{4.49}$$

$$\dot{z}_1 = -55\,\mathrm{sign}(z_0 - \sigma) \tag{4.50}$$

where z_0, z_1 are real-time estimations of $\sigma, \dot{\sigma}$, respectively. The differentiator (4.49), (4.50) is exact for the input signal σ, with a second time derivative not exceeding 50 in absolute value.

The initial conditions $x(0) = \dot{x}(0) = 0$ have been taken as $z_0(0) = x(0) - x_c(0) = -0.5$, $z_1(0) = 0$. The sampling time step τ and the integration step have been chosen as 0.0001.

2-sliding tracking performance and trajectory tracking in the absence of noise, are shown in Fig. 4.13a, b, respectively. The corresponding achieved accuracies are $|\sigma| = |x - x_c| \le 5.4 \times 10^{-6}$, $|\dot{x} - \dot{x}_c| \le 1.0 \times 10^{-2}$ with $\tau = 0.0001$. The control signal associated with Eq. (4.48) is shown in Fig. 4.13c. It is seen from the graph that the control remains continuous until a 2-sliding mode $\sigma = \dot{\sigma} = 0$ takes place. The differentiator convergence is demonstrated in Fig. 4.13d.

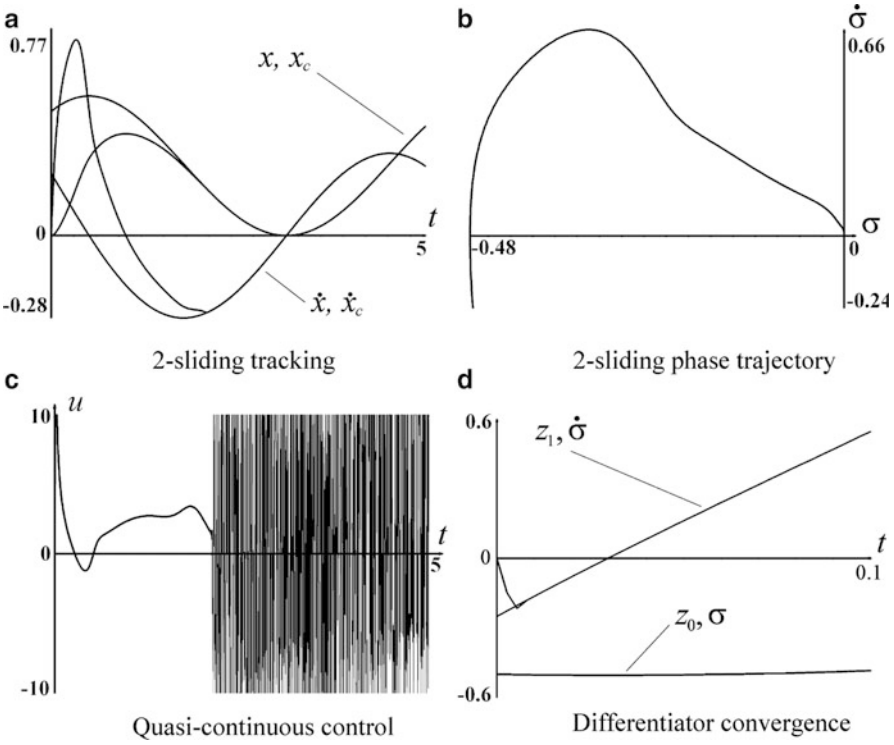

Fig. 4.13 Quasi-continuous pendulum control

The tracking results obtained from using Eqs. (4.48), (4.49), (4.50) and the differentiator performance in the presence of noise with the magnitude 0.01 are demonstrated in Fig. 4.14a, b, respectively. The tracking accuracy is $|\sigma| = |x - x_c| \leq 0.036$ (the noise is a periodic non-smooth function with nonzero average). The performance does not significantly change, when the frequency of the noise varies from $101/s$ to $1000001/s$.

Any other 2-sliding controller could also be implemented. Consider a twisting controller

$$w = -10\,\mathrm{sign}(z_0) - 5\,\mathrm{sign}(z_1) \tag{4.51}$$

The trajectory of the twisting controller (4.49)–(4.51) in the coordinates $x - x_c$ and $\dot{x} - \dot{x}_c$, in the absence of noise, is shown in Fig. 4.15b. The corresponding accuracy is $|x - x_c| \leq 6.7 \times 10^{-6}$, $|\dot{x} - \dot{x}_c| \leq 0.01$.

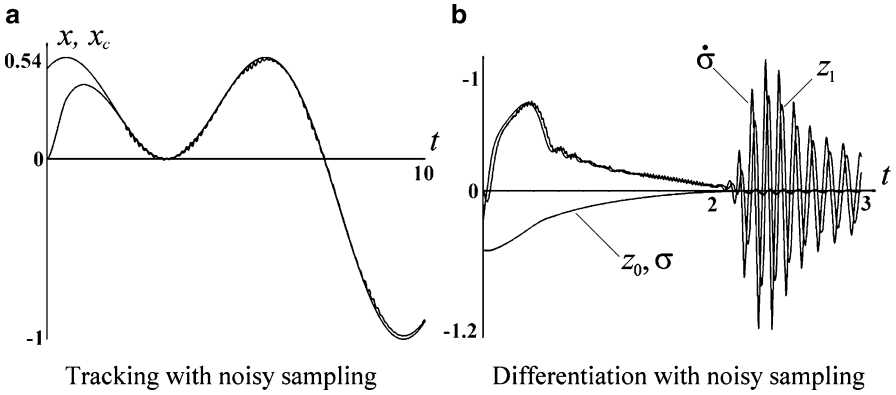

Fig. 4.14 Performance of the quasi-continuous controller with noisy measurements

4.6.2 Chattering Attenuation

In the case when torque chattering is unacceptable, $u = \dot{w}$ is considered as a new control. Define

$$\sigma = (\dot{x} - \dot{x}_c) + 2\,(x - x_c)$$

Again, the relative degree of the system with respect to the new input w is equal 2. Also condition (4.10) holds only locally, and thus the controllers are effective only in a bounded vicinity of the origin $x = \dot{x} = w = 0$. Their global application requires the standard method described in Sect. 4.5, which is not implemented here for simplicity.

The applied output-feedback controller is of the form Eq. (4.42) and is based on the twisting controller (4.13):

$$\dot{w} = u = -15\,\mathrm{sign}\,(z_0) - 10\,\mathrm{sign}(z_1) \tag{4.52}$$

$$\dot{z}_0 = -35\,|z_0 - \sigma|^{1/2}\,\mathrm{sign}\,(z_0 - \sigma) + z_1 \tag{4.53}$$

$$\dot{z}_1 = -70\,\mathrm{sign}\,(z_0 - \sigma)\,,\ \sigma = (\dot{x} - \dot{x}_c) + 2\,(x - x_c) \tag{4.54}$$

Here the angular velocity $\dot{x}$ is assumed to be directly measured.[1]

The initial values $x(0) = \dot{x}(0) = 0$ are taken in the simulations. The value $w(0) = 0$ is taken for controller (4.52)–(4.54), and the sampling step $\tau = 0.0001$. The trajectory in the coordinates $x - x_c$ and $\dot{x} - \dot{x}_c$, in the absence of noise, is shown in Fig. 4.15a. The accuracy $|x - x_c| \le 1.6 \times 10^{-6}$, $|\dot{x} - \dot{x}_c| \le 1.8 \times 10^{-5}$ has been achieved. The trajectories in the presence of noise with magnitude 0.02 in

[1] Otherwise, a 3-sliding controller can be applied together with a second-order differentiator (see chap. 6) producing both $\dot{x} - \dot{x}_c$ and $\ddot{x} - \ddot{x}_c$.

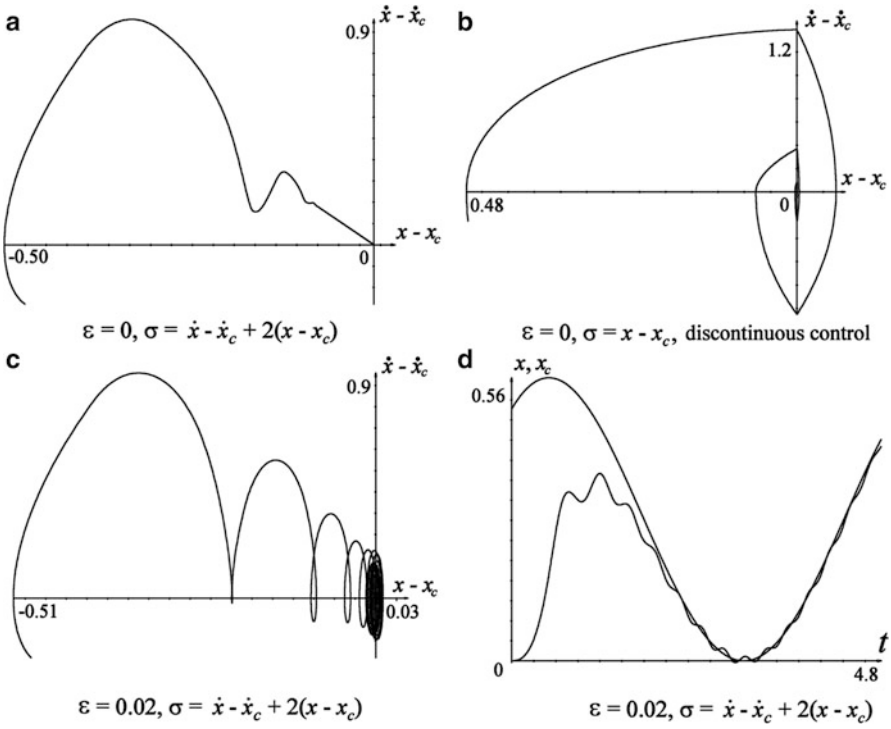

Fig. 4.15 Pendulum output-feedback twisting control, a,c,d: $\sigma = (\dot{x} - \dot{x}_c) + 2(x - x_c)$, b: $\sigma = x - x_c$

the σ-measurements are shown in Fig. 4.15c, and the tracking results are shown in Fig. 4.15d. The tracking accuracy $|x - x_c| \leq 0.018$, $|\dot{x} - \dot{x}_c| \leq 0.16$ is achieved. The performance does not differ when the frequency of the noise changes from $101/s$ to $100001/s$.

4.7 Variable-Gain Super-Twisting Control

An extension of the standard super-twisting algorithm for the conventional two-step SM control design procedure that provides exact compensation of smooth uncertainties/disturbances bounded together with their derivatives by *known functions* is considered in this section.

4.7.1 Problem Statement

Consider a linear time-invariant system (LTI) with a matching nonlinear perturbation

$$\dot{x} = Ax + B(u + \xi(x,t)) \tag{4.55}$$

where $x \in \mathbb{R}^n$ is the state vector, $u \in \mathbb{R}^m$ is the control input, the A and B are constant matrices of appropriate dimensions, and ξ is an absolutely continuous uncertainty/disturbance in the system (4.55). As in Chap. 2 the system in Eq. (4.55) is first transformed into regular form. The following properties are assumed:

(A1) Rank $B = m$.
(A2) The pair (A, B) is controllable.
(A3) The function ξ together with its gradient is bounded by known continuous functions almost everywhere.

Under assumptions (A1) and (A2), after the linear state transformation,

$$\begin{pmatrix} z_1 \\ z_2 \end{pmatrix} = Tx\ ,\ T = \begin{bmatrix} B^{\perp} \\ B^{+} \end{bmatrix}\ ,\ B^{+} = (B^T B)^{-1} B^T\ ,\ B^{\perp} B = 0 \tag{4.56}$$

system (4.55) has the regular form

$$\begin{aligned} \dot{z}_1 &= A_{11} z_1 + A_{12} z_2 \\ \dot{z}_2 &= A_{21} z_1 + A_{22} z_2 + u + \tilde{\xi}\,(z_1, z_2, t) \end{aligned} \tag{4.57}$$

where $z_1 \in \mathbb{R}^{n-m}$ and $z_2 \in \mathbb{R}^m$. The structure of the system allows us, without loss of generality, to restrict ourselves to the single input case ($m = 1$). The results are easily extended to the multi-input case. The sliding surface is chosen to have the form

$$\sigma = z_2 - K z_1 = 0 \tag{4.58}$$

As a consequence, when the motion is restricted to the manifold, the reduced-order model

$$\dot{z}_1 = (A_{11} + A_{12} K)\, z_1 \tag{4.59}$$

has the required performance. Since the pair (A_{11}, A_{12}) is controllable, the matrix K can be designed using any linear control design method for system (4.59); see, for example, Chap. 2.
Using (z_1, σ) as state variables and applying the controller

$$u = -\left(A_{21} + A_{22} K - K\left(A_{11} + A_{12} K\right)\right) z_1 - \left(A_{22} - K A_{12}\right) \sigma + v \tag{4.60}$$

system (4.57) takes the form

$$\dot{z}_1 = (A_{11} + A_{12} K)\, z_1 + A_{12} \sigma \tag{4.61}$$

$$\dot{\sigma} = v + \tilde{\xi}\,(z_1, \sigma + K z_1, t) \tag{4.62}$$

When the perturbation is bounded by a known function $\varrho(x)$

$$|\xi(x,t)| \leq \varrho(x) \tag{4.63}$$

a (first-order) sliding mode can be enforced by a variable-gain controller

$$v = -(\varrho(x) + \varrho_0)\,\mathrm{sign}(\sigma) \tag{4.64}$$

with $\varrho_0 > 0$. Alternatively, unit vector controllers can also be used for this purpose (see Chap. 2). The main disadvantage of these controllers is that they produce *chattering*, which grows with the uncertainty bound $\varrho(x)$.

Here a Lyapunov-based design is employed.

4.7.2 The Variable-Gain Super-Twisting Algorithm

The variable-gain super-twisting algorithm (VGSTA) proposed here is given by

$$v = -k_1(t,x)\,\phi_1(\sigma) - \int_0^t k_2(t,x)\,\phi_2(\sigma)\,dt \tag{4.65}$$

where

$$\begin{aligned} \phi_1(\sigma) &= |\sigma|^{\frac{1}{2}}\,\mathrm{sign}(\sigma) + k_3\sigma \\ \phi_2(\sigma) &= \tfrac{1}{2}\,\mathrm{sign}(\sigma) + \tfrac{3}{2}k_3\,|\sigma|^{\frac{1}{2}}\,\mathrm{sign}(\sigma) + k_3^2\sigma, \quad k_3 > 0 \end{aligned}$$

When $k_3 = 0$ and the gains k_1 and k_2 are constant, we recover the standard super-twisting algorithm. The additional term $k_3 > 0$ allows us to deal with perturbations growing linearly in s, i.e., outside of the sliding surface, and the variable gains k_1 and k_2 make it possible to render the sliding surface insensitive to perturbations growing with bounds given by known functions. Note that the uncertainty/disturbance can always be written as

$$\tilde{\xi}(z_1, \sigma + Kz_1, t) = \underbrace{\left[\tilde{\xi}(z_1, \sigma + Kz_1, t) - \tilde{\xi}(z_1, Kz_1, t)\right]}_{g_1(z_1,\sigma,t)} + \underbrace{\tilde{\xi}(z_1, Kz_1, t)}_{g_2(z_1,t)}$$

where $g_1(z_1, \sigma, t) = 0$, when $\sigma = 0$. It follows from assumption (A3) that the uncertainty/disturbance $\xi(x,t)$ is bounded almost everywhere:

$$\begin{aligned} |g_1(z_1,\sigma,t)| &\leq \varrho_1(t,x)\,|\phi_1(\sigma)| \\ \left|\tfrac{d}{dt}g_2(z_1,t)\right| &\leq \varrho_2(t,x)\,|\phi_2(\sigma)| \end{aligned} \tag{4.66}$$

where $\varrho_1(t,x) \geq 0$, $\varrho_2(t,x) \geq 0$ are known continuous functions.

System (4.62) driven by the VGSTA (4.65) can be written as

$$\begin{aligned} \dot{z}_1 &= (A_{11} + A_{12}K)\, z_1 + A_{12}\sigma \\ \dot{\sigma} &= -k_1(t,x)\,\phi_1(\sigma) + z + g_1(z_1,\sigma,t) \\ \dot{z}_0 &= -k_2(t,x)\,\phi_2(\sigma) + \tfrac{d}{dt} g_2(z_1,t) \end{aligned} \tag{4.67}$$

The algorithm is presented in the following theorem:

Theorem 4.10. *Suppose that for some known continuous functions $\varrho_1(t,x) \geq 0$, $\varrho_2(t,x) \geq 0$ the inequalities (4.66) are satisfied. Then for any initial condition $(z_1(0), \sigma(0), z_0(0))$ the sliding surface $\sigma = 0$ will be reached in finite time if the variable gains are selected as*

$$\begin{aligned} k_1(t,x) &= \delta + \tfrac{1}{\beta}\left(\tfrac{1}{4\epsilon}(2\epsilon\varrho_1 + \varrho_2)^2 + +2\epsilon\varrho_2 + \epsilon + (2\epsilon + \varrho_1)\left(\beta + 4\epsilon^2\right)\right) \\ k_2(t,x) &= \beta + 4\epsilon^2 + 2\epsilon k_1(t,x) \end{aligned} \tag{4.68}$$

where $\beta > 0$, $\epsilon > 0$, $\delta > 0$ are arbitrary positive constants. The reaching time of the sliding surface can be estimated by

$$T = \frac{2}{\gamma_2} \ln\left(\frac{\gamma_2}{\gamma_1} V^{\frac{1}{2}}(\sigma(0), z_0(0)) + 1\right) \tag{4.69}$$

where $V(\sigma, z_0) = \zeta^T P \zeta$, with $\zeta^T = \left[|\sigma|^{\frac{1}{2}} sign(\sigma) + k_3\sigma\ ,\quad z_0\right]$ and

$$\gamma_1 = \frac{\epsilon\lambda_{\min}^{\frac{1}{2}}\{P\}}{\lambda_{\max}\{P\}},\ \gamma_2 = \frac{2\epsilon k_3}{\lambda_{\max}\{P\}} \tag{4.70}$$

Proof. We will show that the quadratic form

$$V(\sigma, z_0) = \zeta^T P \zeta \tag{4.71}$$

where

$$\zeta^T = \left[|\sigma|^{\frac{1}{2}} \operatorname{sign}(\sigma) + k_3\sigma\ ,\quad z_0\right] \tag{4.72}$$

and

$$P = \begin{bmatrix} p_1 & p_3 \\ p_3 & p_2 \end{bmatrix} = \begin{bmatrix} \beta + 4\epsilon^2\ , & -2\epsilon \\ -2\epsilon & 1 \end{bmatrix} \tag{4.73}$$

with arbitrary positive constants $\beta > 0$, $\epsilon > 0$, is a Lyapunov function for the subsystem (σ, z_0) of Eq. (4.67), showing finite-time convergence. Function (4.71) is positive definite, everywhere continuous, and differentiable everywhere except on the set $\mathcal{S} = \left\{(\sigma, z_0) \in \mathbb{R}^2 \mid \sigma = 0\right\}$. The inequalities (4.66) can be rewritten as $g_1(z_1,\sigma,t) = \alpha_1(t,x)\,\phi_1(\sigma)$ and $\frac{d}{dt} g_2(z_1,t) = \alpha_2(t,x)\,\phi_2(\sigma)$ for some

functions $|\alpha_1(t,x)| \leq \varrho_1(t,x)$ and $|\alpha_2(t,x)| \leq \varrho_2(t,x)$. Using these functions and noting that $\phi_2(\sigma) = \phi_1'(\sigma)\phi_1(\sigma)$ one can show that

$$\begin{aligned}\dot{\zeta} &= \begin{bmatrix} \phi_1'(\sigma)\{-k_1(t,x)\phi_1(\sigma) + z_0 + g_1(x,t)\} \\ -k_2(t,x)\phi_2(\sigma) + \frac{d}{dt}g_2(x,t) \end{bmatrix} \\ &= \phi_1'(\sigma)\begin{bmatrix} -(k_1(t,x)-\alpha_1(t,x)) \ , & 1 \\ -(k_2(t,x)-\alpha_2(t,x)) & 0 \end{bmatrix}\zeta = \phi_1'(\sigma)\mathcal{A}(t,x)\zeta\end{aligned}$$

for every point in $\mathbb{R}^2\backslash\mathcal{S}$, where this derivative exists. Similarly one can calculate the derivative of $V(x)$ on the same set as

$$\begin{aligned}\dot{V}(\sigma,z_0) &= \phi_1'(\sigma)\zeta^T\left(\mathcal{A}^T(t,x)P + P\mathcal{A}(t,x)\right)\zeta \\ &= -\phi_1'(\sigma)\zeta^T Q(t,x)\zeta\end{aligned}$$

where

$$Q(t,x) = \begin{bmatrix} 2(k_1(t,x)-\alpha_1)p_1 + 2(k_2(t,x)-\alpha_2)p_3 & \bigstar \\ (k_1(t,x)-\alpha_1)p_3 + (k_2(t,x)-\alpha_2)p_2 - p_1 \ , & -2p_3 \end{bmatrix}$$

Selecting P as in Eq. (4.73) and the gains as in Eq. (4.68), we have

$$\begin{aligned}Q - 2\epsilon I &= \begin{bmatrix} 2\beta k_1 + 4\epsilon(2\epsilon k_1 - k_2) - 2\left(\beta + 4\epsilon^2\right)\alpha_1 + 4\epsilon\alpha_2 - 2\epsilon & \bigstar \\ k_2 - 2\epsilon k_1 - \left(\beta + 4\epsilon^2\right) + 2\epsilon\alpha_1 - \alpha_2 \ , & 2\epsilon \end{bmatrix} \\ &= \begin{bmatrix} 2\beta k_1 - \left(\beta + 4\epsilon^2\right)(4\epsilon + 2\alpha_1) + 4\epsilon\alpha_2 - 2\epsilon & \bigstar \\ 2\epsilon\alpha_1 - \alpha_2 \ , & 2\epsilon \end{bmatrix}\end{aligned}$$

that is positive definite for every value of (t,x). This shows that

$$\dot{V} = -\phi_1'(\sigma)\zeta^T Q(t,x)\zeta \leq -2\epsilon\phi_1'(\sigma)\zeta^T\zeta = -2\epsilon\left(\frac{1}{2|\sigma|^{\frac{1}{2}}} + k_3\right)\zeta^T\zeta$$

Since $\lambda_{\min}\{P\}\|\zeta\|_2^2 \leq \zeta^T P\zeta \leq \lambda_{\max}\{P\}\|\zeta\|_2^2$, where

$$\|\zeta\|_2^2 = \zeta_1^2 + \zeta_2^2 = |\sigma| + 2k_3|\sigma|^{\frac{3}{2}} + k_3^2\sigma^2 + z_0^2$$

is the Euclidean norm of ζ, and

$$|\zeta_1| \leq \|\zeta\|_2 \leq \frac{V^{\frac{1}{2}}(\sigma,z_0)}{\lambda_{\min}^{\frac{1}{2}}\{P\}}$$

we can conclude that

$$\dot{V} \leq -\gamma_1 V^{\frac{1}{2}}(\sigma, z_0) - \gamma_2 V(\sigma, z_0)$$
$$\gamma_1 = \frac{\epsilon \lambda_{\min}^{\frac{1}{2}}\{P\}}{\lambda_{\max}\{P\}},\ \gamma_2 = \frac{2\epsilon k_3}{\lambda_{\max}\{P\}} \tag{4.74}$$

Note that the trajectories cannot stay on the set $\mathcal{S} = \left\{(\sigma, z_0) \in \mathbb{R}^2 \mid \sigma = 0\right\}$. This means that V is a continuously decreasing function and we can conclude that the equilibrium point $(\sigma, z_0) = 0$ is reached in finite time from every initial condition.[2]

Since the solution of the differential equation

$$\dot{v} = -\gamma_1 v^{\frac{1}{2}} - \gamma_2 v\,, \quad v(0) \geq 0$$

is given by

$$v(t) = \exp(-\gamma_2 t)\left[v(0)^{\frac{1}{2}} + \frac{\gamma_1}{\gamma_2}\left(1 - \exp\left(\frac{\gamma_2}{2}t\right)\right)\right]^2$$

it follows that $(\sigma(t), z_0(t))$ converges to zero in finite time and reaches that value at most after a time given by Eq. (4.69). This concludes the proof of Theorem 4.10. □

Remark 4.7. Theorem 4.10 proposes a methodology to design a sliding mode controller ensuring a sliding motion on the surface (4.58) substituting the discontinuous control law (4.64) by an absolutely continuous VGSTA (4.65). In this case the chattering level can be substantially reduced.

When $\rho(x) = const$, first-order sliding mode controllers (4.64) are able to compensate the bounded perturbations $\xi(x(t), t)$ measurable along the system trajectories. On the other hand the super-twisting algorithm with constant gains k_1 and k_2 is able to compensate for the Lipschitz continuous perturbations $\xi(x, t)$ along the system trajectories, but their absolute value cannot grow faster than a linear function of t, nor faster than linear with respect to $|\sigma(t)|^{\frac{1}{2}}$ along the system trajectories. Theorem 4.10 extends the VGSTA design for the class of perturbations (4.66).

[2] For details see Zubov's stability theorem [196].

4.8 Case Study: The Mass–Spring–Damper System

4.8.1 Model Description

The mass–spring–damper (MSD) system consists of two masses, three springs, one damper, and a DC motor in the configuration shown in Fig. 4.16. The system is the Educational Control Products (ECP) model 210a.

The dynamics of the system are given by the following set of ordinary differential equations:

$$m_2\ddot{\chi}_2 + (\kappa_3 + \kappa_2)\chi_2 + c_1\dot{\chi}_2 - \kappa_2\chi_1 = 0 \tag{4.75}$$

$$m_1\ddot{\chi}_1 + (\kappa_1 + \kappa_2)\chi_1 - \kappa_2\chi_2 = F \tag{4.76}$$

where $\chi_1, \dot{\chi}_1, \ddot{\chi}_1, \chi_2, \dot{\chi}_2, \ddot{\chi}_2$ are the position, velocity, and acceleration of the masses 1 and 2, respectively. The term F is the force that the DC motor inputs into mass 1. The state vector is selected as $x_1 = \chi_1$, $x_2 = \dot{\chi}_1$, $x_3 = \chi_2$, and $x_4 = \dot{\chi}_2$, and the input $u = F$. The state space representation is

$$\dot{x_1} = x_2 \tag{4.77}$$

$$\dot{x_2} = -\frac{\kappa_1}{m_1}x_1 - \frac{\kappa_2}{m_1}x_1 + \frac{\kappa_2}{m_1}x_3 + \frac{1}{m_1}u \tag{4.78}$$

$$\dot{x_3} = x_4 \tag{4.79}$$

$$\dot{x_4} = -\frac{(\kappa_3 + \kappa_2)}{m_2}x_3 - \frac{c_1}{m_2}x_4 + \frac{\kappa_2}{m_2}x_1 \tag{4.80}$$

The nominal values are shown in Table 4.1.
It is possible to measure the positions x_1, x_3 through the encoders that are coupled to mass 1 and mass 2 respectively.

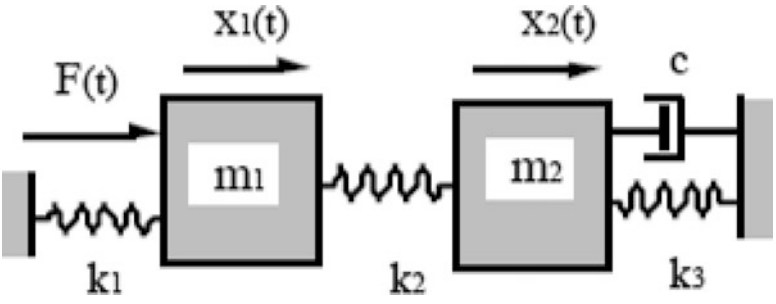

Fig. 4.16 The mass–spring–damper (MSD) system

Table 4.1 Model Nominal Values

Name	m_1	m_2	κ_1	κ_2	κ_3	c_1
Value	1.28	1.05	190	780	450	15
Units	$[kg]$	$[kg]$	$[N/m]$	$[N/m]$	$[N/m]$	$[N \cdot s/m]$

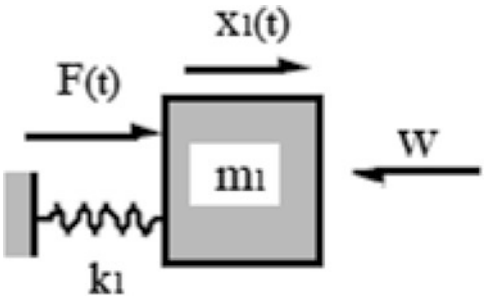

Fig. 4.17 The mass–spring system with disturbance

4.8.2 Problem Statement

To design the control we will consider just the mass m_1 and the spring κ_1 as part of the system and everything else is considered a disturbance as shown in Fig. 4.17. This configuration yields the state-space representation

$$\dot{x_1} = x_2 \tag{4.81}$$

$$\dot{x_2} = -\frac{\kappa_1}{m_1}x_1 + \frac{1}{m_1}(u + w) \tag{4.82}$$

where

$$w = \kappa_2(x_3 - x_1) \tag{4.83}$$

The goal of the control is to track the desired position $[x_d, 0]^T$ where x_d is constant. To work at the equilibrium point instead of the point $[x_d, 0]^T$ the following change of coordinates can be applied:

$$\begin{bmatrix} \bar{x}_1 \\ \bar{x}_2 \end{bmatrix} = \begin{bmatrix} x_1 - x_d \\ x_2 \end{bmatrix}$$

and using the control law $u = \kappa_1 x_d + u_1$ we can obtain the system

$$\dot{\bar{x}}_1 = \bar{x}_2 \tag{4.84}$$

$$\dot{\bar{x}}_2 = -\frac{\kappa_1}{m_1}\bar{x}_1 + \frac{1}{m_1}(u_1 + w) \tag{4.85}$$

such that when $\bar{x} = 0$ then $[x_1, x_2]^T = [x_d, 0]^T$. System (4.85) satisfies assumptions (A1) and (A2) and therefore it can be transformed to the regular form using Eq. (4.56) so that

$$\begin{bmatrix} z_1 \\ z_2 \end{bmatrix} = \begin{bmatrix} b & 0 \\ 0 & b^{-1} \end{bmatrix} \begin{bmatrix} \bar{x}_1 \\ \bar{x}_2 \end{bmatrix} \tag{4.86}$$

where $b = \frac{1}{m_1}$. Using Eq. (4.56), system (4.85) is transformed into

$$\dot{z}_1 = b^2 z_2 \tag{4.87}$$

$$\dot{z}_2 = -\frac{\kappa_1}{b} z_1 + u_1 + w \tag{4.88}$$

The control aim now is to stabilize the origin of system.

4.8.3 Control Design

Let us design the sliding surface as

$$\sigma = z_2 + K z_1 \tag{4.89}$$

such that when the motion is restricted to the manifold, the reduced-order dynamics will have the desired performance

$$\dot{z}_1 = -b^2 K z_1$$

and the desired value will be tracked exponentially

$$z_1 = C_1 e^{-K b^2 t}$$

Secondly we want to change the state variables (z_1, z_2) to (z_1, σ). Taking into account (4.89) we can write z_2 as

$$z_2 = \sigma - K z_1 \tag{4.90}$$

and $\dot{\sigma}$ as

$$\dot{\sigma} = \dot{z}_2 + K \dot{z}_1 \tag{4.91}$$

Then using Eqs. (4.90) and (4.91) we can easily construct the input

$$u_1 = -K(-b^2 K z_1 + b^2 \sigma) + \frac{\kappa_1}{b} z_1 + v \tag{4.92}$$

that will transform the system into

$$\dot{z}_1 = -b^2 K z_1 + b^2 \sigma \tag{4.93}$$

$$\dot{\sigma} = v + w \tag{4.94}$$

where v is the virtual control established in Eq. (4.65). To select the bounds for the disturbance, we can write (4.83) in terms of (z_1, σ) as

$$w(t, z_1) = \kappa_2 x_3(t) - \kappa_2 b z_1 \tag{4.95}$$

where the term $x_3(t)$ is considered as exogenous, and only x_1 belongs to system (4.82). From Eq. (4.95) we can obtain the terms g_1 and g_2 as

$$g_1(z_1, \sigma, t) = 0 \tag{4.96}$$

$$g_2(z_1, t) = \kappa_2 x_3(t) - \kappa_2 b z_1 \tag{4.97}$$

$$\frac{dg_2(z_1, t)}{dt} = \kappa_2 x_4(t) - \kappa_2 b \dot{z}_1 \tag{4.98}$$

$$\frac{dg_2(z_1, t)}{dt} = \kappa_2 x_4(t) - \kappa_2 b(b^2\sigma - b^2 K z_1) \tag{4.99}$$

Next ϱ_1 and ϱ_2 are selected to accomplish the restriction (4.66). Since $|\varphi_2(\sigma)| > \frac{1}{2}$ everywhere except on $\sigma = 0$ we can select ϱ_1 and ϱ_2 as follows $\varrho_1 = 0$ and

$$\varrho_2 = 2[\kappa_2 x_4(t) - \kappa_2 b(b^2\sigma - b^2 K z_1)] \tag{4.100}$$

Finally we use the inverse transform

$$\begin{bmatrix} 0 \\ b \end{bmatrix} u_1 \quad = \quad T^{-1} \begin{bmatrix} 0 \\ 1 \end{bmatrix} u_1$$

4.8.4 *Experimental Results*

The total time of the experiment was $10[s]$ and the desired position was $x_d = 1[cm]$, This position is demanded when $t = 0.5[s]$. The parameters δ, β, and ϵ of the variable gains k_1 and k_2 and the fixed gain k_3 are selected as $\delta = 0.001$, $\beta = 4.1$, $\epsilon = 0.11$, and $k_3 = 8$, and the parameter K from the sliding surface (4.89) is selected as $K = 3$. The reference x_d is reached despite the disturbance as can be seen in Figs. 4.18 and 4.19. Chattering is completely eliminated (see Fig. 4.18). This result is achieved with a sampling time of $T_s = 1[ms]$. The behavior of σ is shown in Fig. 4.20 and the VGSTA output is shown in Fig. 4.21.

4.9 Notes and References

The twisting controller [75, 132] was historically the first 2-sliding mode controller to be proposed. The suboptimal controller appears first in [18, 20]. The controller with prescribed convergence law was proposed in [75, 132]. The quasi-continuous control algorithm is proposed in [127, 128]. In the particular case when

$$u = -\alpha \operatorname{sign}\left(\dot{\sigma} + \beta |\sigma|^{1/2} \operatorname{sign}(\sigma)\right), \quad \alpha, \beta > 0, \ \alpha K_m - C > \beta^2/2 \tag{4.101}$$

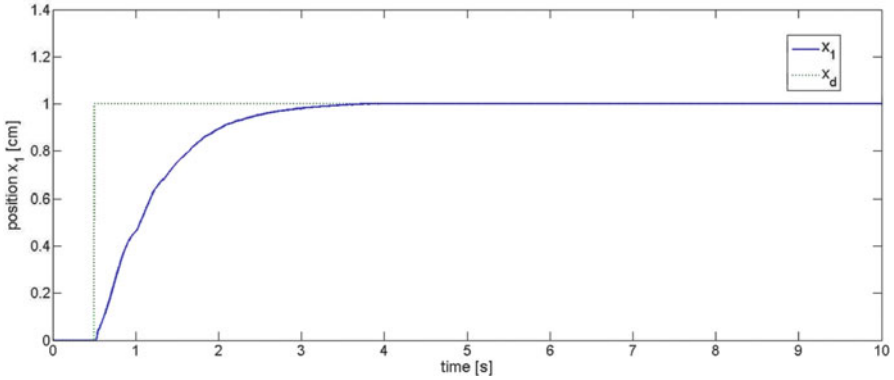

Fig. 4.18 Output of the system tracking $x_d = 1[cm]$

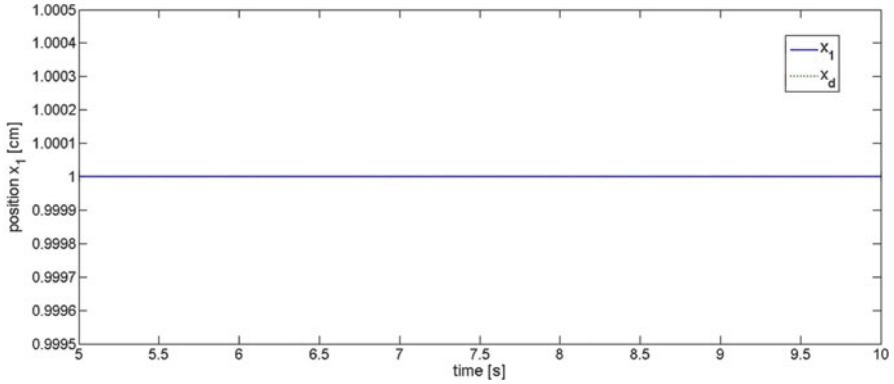

Fig. 4.19 Zoom of the system output tracking $x_d = 1[cm]$

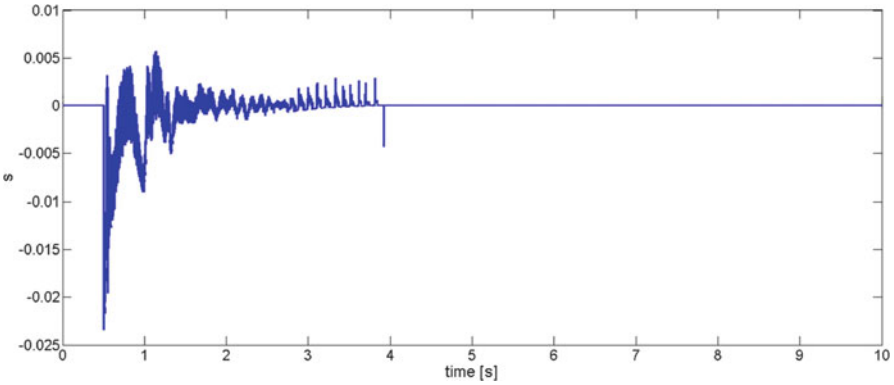

Fig. 4.20 The sliding surface

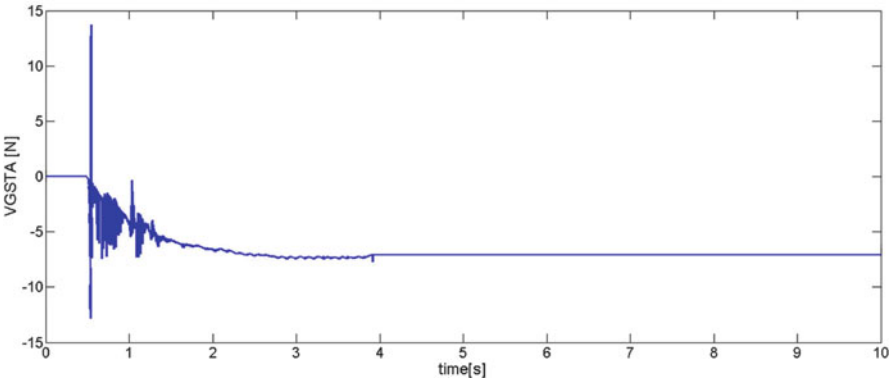

Fig. 4.21 The output of the VGSTA

the controller given in Eq. (4.101) is similar to so-called terminal sliding mode controllers [138]. An alterative detailed proof of Theorem 4.2 can be found in [17].

The long-standing concern associated with conventional sliding mode control is the attenuation of the so-called chattering effect. Many different approaches have been suggested: see, for example, [29, 31, 87–90, 98, 171]. However, 2-sliding mode control ideas provide effective tools for the reduction or even practical elimination of the chattering without compromising the benefits of conventional sliding modes: see, for example, [18,20,31,33–35,125,132]. Additional information about 2-sliding mode controllers and differentiators can be in [15, 16, 19, 122, 153].

Theorem 4.8 is based on the results presented in [123]. The accuracy estimations formulated in Theorem 4.8 remain valid in the presence of sufficiently small noise and/or sampling intervals. Note that although Theorem 4.9 is not formulated for arbitrary 2-sliding homogeneous controllers, it is valid for all standard 2-SM controllers [20, 132]. It can be shown that the chattering phenomenon is indeed mitigated by means of this procedure. Moreover, noise caused by unaccounted-for fast stable actuators and sensors does not produce chattering. Theorem 4.10 extends the Lyapunov-based design method from [142] for the standard twisting algorithm in order to include (i) linear (nonhomogeneous) terms and (ii) variable gains, in order to alleviate the drawbacks of the standard twisting algorithm. The use of the Lyapunov method is instrumental here, since neither geometric or homogeneity based proofs can be used to deal with these extensions [12, 126]. Section 4.9 presents the results of the paper [101]. It is a particular case of the Lyapunov-based approach to the second-order sliding mode control design presented by Moreno in [142, 143]. Based on this approach fixed-time convergent controllers and differentiators [51, 152] are developed ensuring a uniform convergence time with respect to initial conditions. Such algorithms being applied to hybrid and switched systems with strictly positive dwell-time can ensure the convergence of observers and controllers before the system jumps of switches.

4.10 Exercises

Exercise 4.1. Prove the local asymptotic convergence of the trajectories of Eqs. (4.1), (4.3) to the 2-sliding mode $x = 0, u = 1/2$ for any $a > 2$.

Hint: consider the Lyapunov function $V(x) = |x| + \frac{1}{2a}(u - \sin(x + \pi/6))$.

Exercise 4.2. List all the controllers from Sect. 4.2 capable of making the output x of the perturbed pendulum $\ddot{x} = \sin(x) + f(t) + u, |f(t)| \leq 1$ exactly follow any real-time available function $x_c(t)$ with $|\ddot{x}_c| \leq 1$.

Exercise 4.3. Locally solve the previous problem with $|\dot{x}| < 2$ to provide asymptotically exact tracking by means of continuous control, using the super-twisting controller. Assume the additional conditions $\left|\dot{f}\right| \leq 1, |\dddot{x}_c| \leq 2; \dot{x}$ hold. Hint: Keep the constraint $\dot{x} + x = 0$.

Exercise 4.4. Solve the previous problem of asymptotically exact tracking, by means of continuous control, using the controllers from Sect. 4.2. Both $\dot{x}$ and $\ddot{x}$ are assumed to be available.

Exercise 4.5. Choose the parameters of the differentiator (4.38), (4.39) to facilitate the exact differentiation of the signal $f = \cos(2(3t - 5)) + 4t$.

Exercise 4.6. Check the solution of the previous problem by means of computer simulation. Introduce arbitrary noise of the magnitude 0.01 and check the robustness of the differentiator in the presence of nosie of different frequencies (e.g., one can take the "noise" $0.01sin(\omega t)$ or any other periodic function, even discontinuous).

Exercise 4.7. Solve problems 4.2, 4.3 by means of output-feedback controllers.

Exercise 4.8. Solve problem 4.4 using a differentiator assuming that $\dot{x}$ is available.

Exercise 4.9. Verify the solutions of problems 4.7, 4.8 by computer simulation. In addition introduce small measurement noise.